109

A LOW FREQUENCY UNDERWATER SOUND PROPAGATION MODEL

by

MARTHINUS PETRUS STANDER

Submitted in fulfilment of the
requirements for the degree of
Master of Science
(Physical oceanography)

UNIVERSITY OF CAPE TOWN

November 1993

ABSTRACT

All wave-theoretic underwater sound propagation models attempt to derive the acoustic field originating from a sound source in a specific environment by either solving the wave equation directly or by solving an approximation there-of.

This dissertation describes a normal mode direct solution with emphasis on the application as well as the theoretic analysis capability of the specific model, called NORMAN.

ACKNOWLEDGEMENTS

I would like to take this opportunity to thank Professor G.B. Brundrit, my supervisor, for his guidance and support throughout my study.

Sincere thanks are also extended to Ms S. Eva and the Institute for Maritime Technology for their contribution towards the creation of this report.

TABLE OF CONTENTS

LIST OF ILLUSTRATIONS

CHAPTER 1: INTRODUCTION

"At present, the available computer programs are restricted to those which use ray methods to simulate high frequency sound propagation in range-independent oceanic environments. Such simulations take no account of the rich frontal structures of the waters of the South African continental shelf, as revealed by field exercises of recent years. Nor can the programs be used for the propagation of low frequency sound, with its potential for greater overall range.

Progress beyond the present capability can only be made by moving beyond ray methods into the realm of full wave methods."

This quotation from an internal report at the Institute for Maritime Technology in Simon's Town South Africa in 1990, identified a major technology shortcoming in the local underwater sound propagation modelling capability at that time. The result of this gap was far reaching and when translated to specific drawbacks simply meant that although the advantage of utilising low frequency sound propagation was recognized and that internationally it was a popular field of study, even very basic wave theoretic principles were not understood. This implied that it was not possible to predict low frequency underwater sound propagation, nor to use low frequency related hardware with an adequate degree of confidence. Finally, and perhaps most frustratingly, this inadequate level of competence did not allow any participation in, or contribution to the international field of underwater acoustic modelling.

In recent years, innovative approximations to the governing wave equation have led to the development of a hierarchy of numerical techniques as can be seen in figure 1.1.

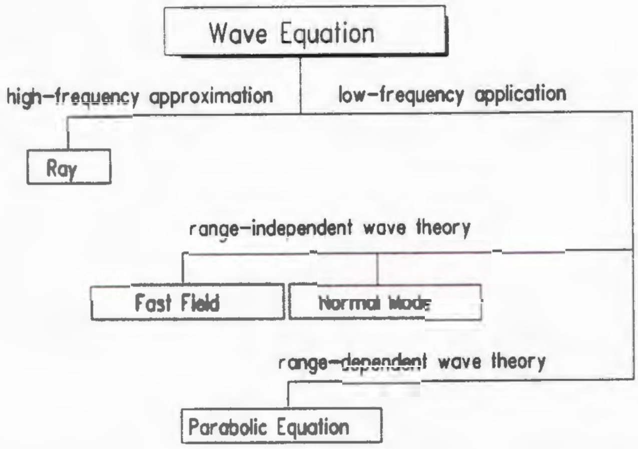

Figure 1.1: Hierarchy of the basic numerical techniques for solving the wave equation ([5]).

In a range-independent environment, the full wave equation is separable and the solution can be represented for the cylindrically spreading far field in terms of normal modes for the vertical structure of the sound field. At low frequencies a limited and computationally manageable number of normal modes are needed. In a different approach, the geometry of the oceanic environment as a small aperture cylinder can be used to approximate the wave equation with a numerically simpler parabolic equation. Range dependent features can then be introduced. Modern versions of this method also do not suffer from the small aperture limitation.

Only high frequency ray approximations have been utilised in the local environment. Such use has provided a very visual insight into studying sound propagation in the ocean.

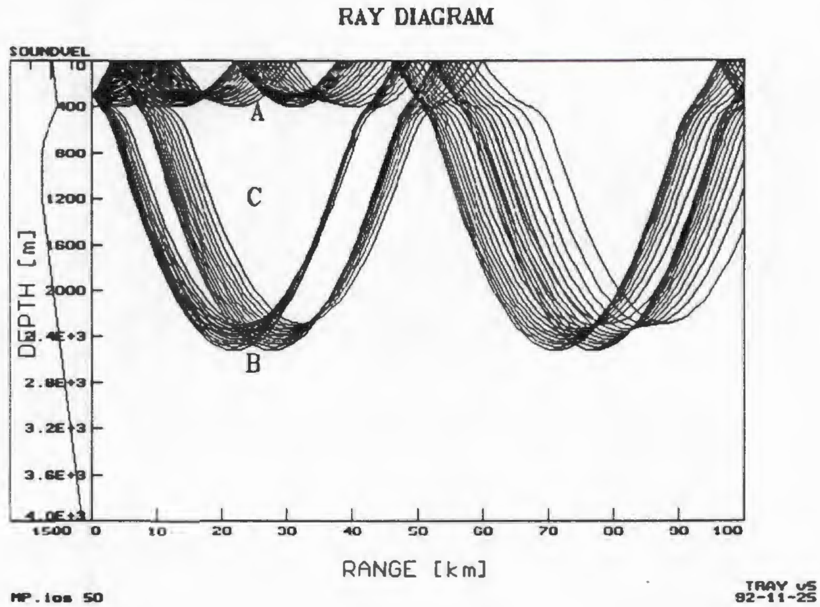

Figure 1.2: A deep water ray diagram of sound propagation ([20]).

The above ray diagram in figure 1.2 illustrates the variable results of sound propagation at a distance, with a slight variance in propagation properties having a large effect on sound intensity distribution. This implies that sound from a fixed source can reach receivers placed in adjacent regions with remarkable differences in intensity. So will a receiver at either position A or B in figure 1.2 be in a favourable region for sound reception while a receiver at C will be in a sound "shadow" region. From this description the importance of being able to predict and model the occurrence of these regions should be clear.

However, general ray theory, which can be described as a continual application of Snell's law in a horizontally stratified medium ([22]), does not include diffraction and other wave effects and therefore fails in adequately describing low frequency ducted propagation as well as significant bottom interaction as is encountered in shallow water.

With a local ocean environment then predominantly being described as shallow water due to the wide continental shelf, and with an underwater acoustic modelling capability limited to ray theory and high frequency, a careful analysis in 1991 based on specific features of different wave theoretic approaches (normal modes, parabolic equation etc.) led to a decision to develop a normal mode sound propagation model locally. Specifically in favour of the normal mode technique was its inherent ability in coping with a shallow water cylindrical spreading environment.

Together with the locally developed ray theory model TRAY ([20]), this development was to provide a local modelling capability which could basically span the complete frequency and water depth range. How well this was achieved is evident from figure 1.3 where it can be seen that the normal mode choice, apart from a limited capability regarding low frequency applications in a range-dependent shallow water environment, fully complements the existing ray theory modelling.

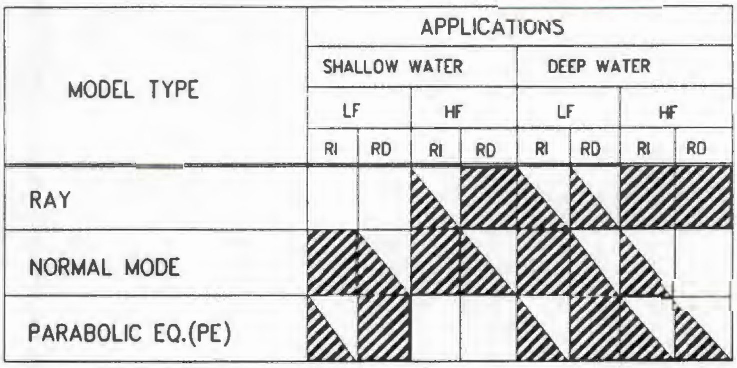

Figure 1.3: Applicability of propagation models ([5]).

The specific normal mode direct solution of the wave equation, called NORMAN, is now presented. Against the historical background of local experience, the original study objectives can be formulated as:

(i) Acquiring a better understanding of low frequency sound propagation in an oceanic environment.

(ii) Providing a functional and practical low frequency underwater sound propagation computer model to the local underwater acoustical community in order to acquire a prediction capability regarding low frequency sound propagation properties in an coastal oceanic environment.

The thesis itself is intended as a measure of how and how well these study objectives were achieved. This is done by documenting the newly gained knowledge, by documenting model NORMAN itself, and by showing how NORMAN can be applied usefully. In other words a *theory-modelling-experiment* approach is taken.

To this effect, chapter 2 is devoted to the concept and theory of normal modes by making use of the ray theory analogy. A transmission loss calculation is also performed. In order to acquaint the reader with NORMAN itself, chapter 3 provides detail of the program input parameters as well as program composition. Examples of all possible output are given and benchmark tests against other international models are provided. Chapter 4 then aims to highlight the versatile application of NORMAN and mode theory. The specific examples are aimed at showing how the local user can now study low frequency underwater sound propagation for the first time. Subjects investigated include the sensitivity of model predictions in a range dependent environment; ducted sound propagation in the deep sound channel as well as in a surface duct; an optimum frequency analysis with regards to minimum loss over propagation range as a function of frequency; a low frequency sonar application involving a seabed transducer array and finally, the result of a local low frequency sound propagation experiment in shallow water is compared to a NORMAN transmission loss prediction.

It is hoped and believed that this intentional blend of general mode theory with specific model detail, certainly unique in a local context, will not only contribute to the knowledge of the interested reader, but will also provide the potential model user with ample information and insight for the proper use of model NORMAN.

CHAPTER 2: NORMAL MODE THEORY

2.1 Introduction

Without going into too much theoretical detail, the aim of this chapter is to highlight enough normal mode theory necessary in order to complement the practical application in chapter 4 as well as the specific model detail in chapter 3.

2.2 Normal modes and ray theory

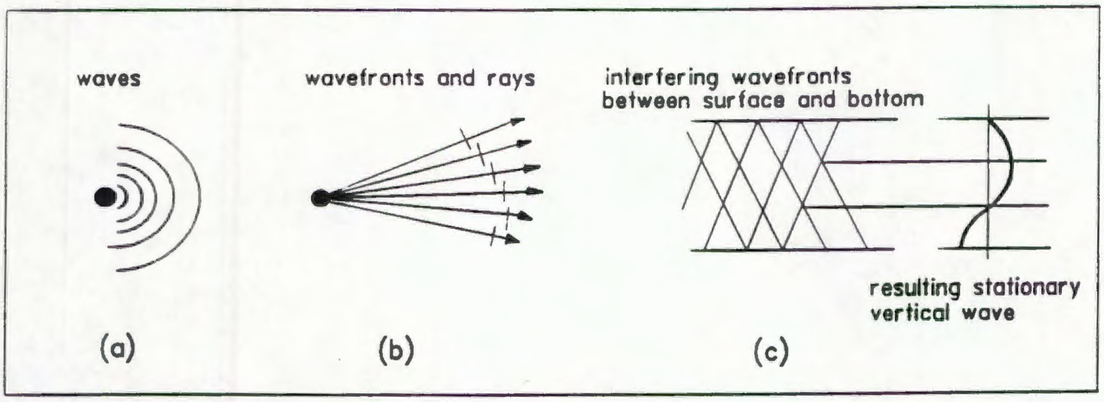

Figure 2.1: Wave- and ray theory of acoustics.

Intuitively as well as visually, ray theory lends itself very well to explaining the basic concepts of underwater sound propagation. In attempting to explain normal modes, the connection between the two theories will be pointed out. In fact, acoustic ray theory evolved as a mathematical approximation to wave theory.

In figure 2.1(a) a sound source gives origin to plane waves which radiate energy from the source centre. This happens because elements of a single wave front acts as sources of new waves (Huygen's wave principle, [18]). This is none other than the so-called "wave theory" in an an elastic medium. Rays are then formed by drawing normal lines from the source through the wave fronts, as in figure 2.1(b).

The wave fronts interfere so that complex depth functions (eigen-functions) can be formed (figure 2.1(c)). These vertical stationary waves are then called the normal or natural modes of the system due to source excitation. The normal mode approach thus basically involves expanding the solution to the wave equation in terms of normal modes in the vertical (indicating pressure and distribution) and cylindrically spreading waves in the horizontal.

Before the mode and ray analogy is continued, the concept of a sound velocity profile should be explained. Underwater sound velocity generally decreases with a depth increase due to the water becoming colder. In the region closer to the surface the velocity is however susceptible to daily and local changes of heating, cooling and wind action and may therefore also exhibit an increase with increasing water depth. In deeper water the sound velocity finally reaches a minimum and thereafter increases with depth due to increasing pressure. Such a SVP as can be seen in figure 2.2 then has a drastic influence on underwater sound propagation and is always vital input information to any sound propagation model.

From figures 2.2 and 2.3 the following mode characteristics can now be noted:

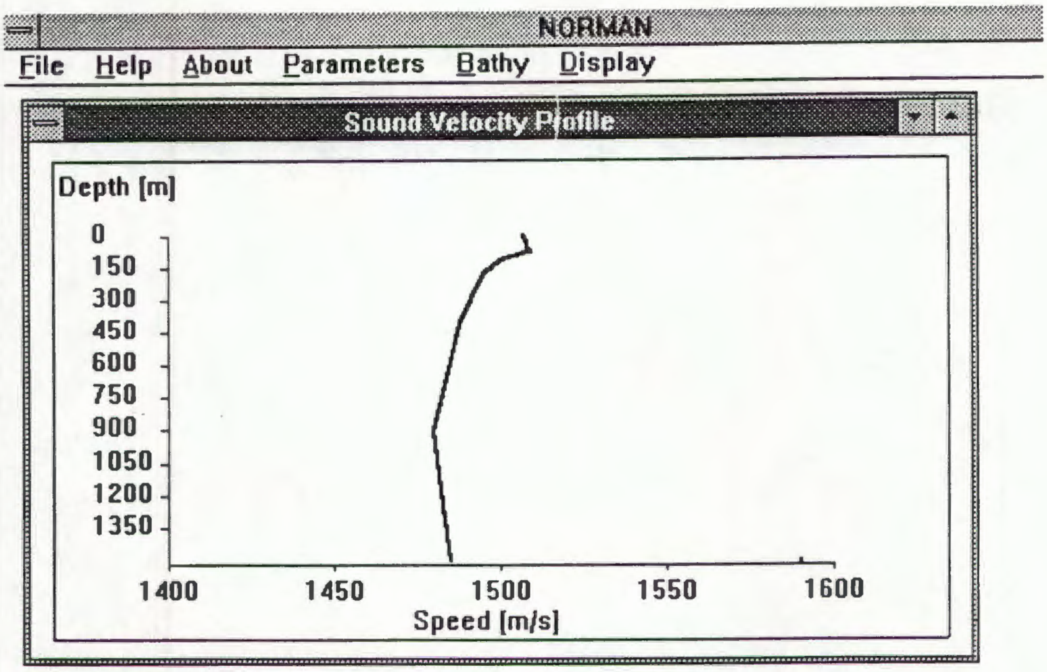

Figure 2.2: A sound velocity profile.

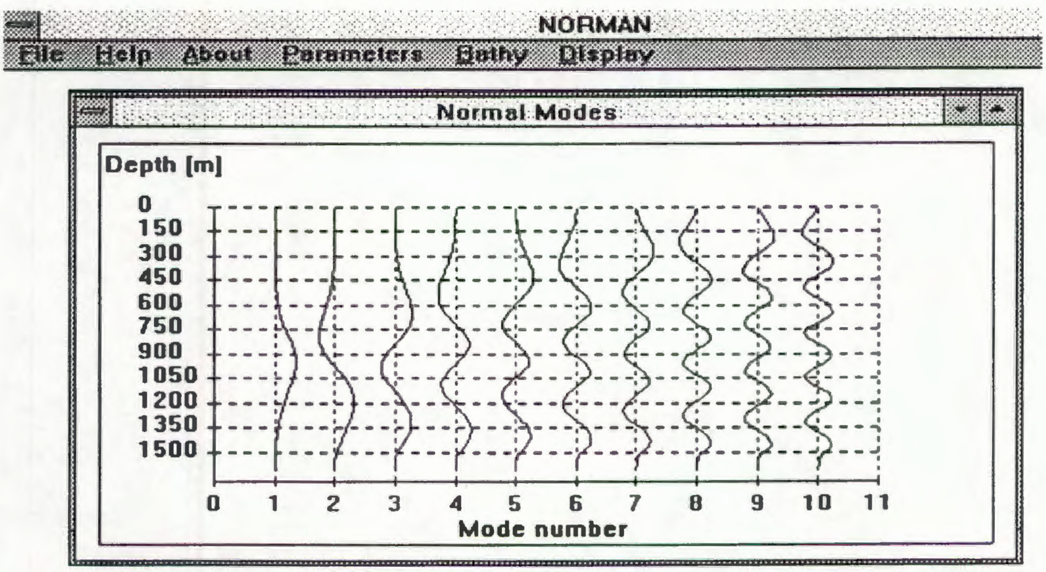

Figure 2.3: Normal modes corresponding to the SVP in figure 2.2 calculated by NORMAN.

- The mode number is associated with the number of maxima or minima of the vertical standing-wave pattern.

- Each mode has a distinctive propagation velocity which varies between the minimum SVP-speed for the lowest mode and the maximum SVP-speed for the highest available mode.

- The modes satisfy boundary conditions, e.g. zero pressure at the surface due to a "pressure release" surface condition.

- Each mode has a distinctive grazing angle which increases with mode number. Higher order modes are therefore more strongly attenuated due to surface and bottom interaction, similar to a steeper ray. It further implies that, if a substantial vertical beam width is required, care must be taken to place the source at a depth which will activate the higher order modes (see test case 1 in chapter 3.). From figure 2.3 it can be seen that from mode 5 the modes "carry" energy into the sediment (below 1500m) due to their increasing grazing angles.

- In a range-independent scenario, the initial mode distribution stays constant across the complete analysis range.

- If a source is situated at the null of a mode, that particular mode will not be activated.

Each normal mode (eigenfunction) also has a distinctive modal wave number (eigenvalue) which becomes complex when attenuation occurs. The normal mode solution can therefore be used to calculate sound propagation loss.

2.3 The wave equation

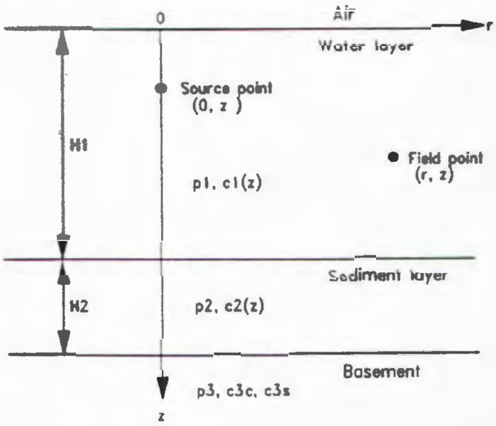

Figure 2.4: A physical model for defining the wave equation ([1]).

In figure 2.4 a physical environment is specified in order to define the wave equation for a normal mode solution applicable to the underwater sound propagation problem.

Two fluid layers, bounded above by air and having respective depths H_1 and H_2, densities ρ_1 and ρ_2, and a third semi-infinite layer of density ρ_3, compressional velocity c_{CB}, and shear velocity c_{SB} (if a solid) make up an infinite half-space in figure 2.4. Variable sound velocity (compressional) profiles are allowed in the fluid layers, $c_1(z)$ and $c_2(z)$. Note that a cylindrical coordinate system in the polar coordinates r and z with azimuthal symmetry assumed (no θ dependency) is established. (See appendix C for a glossary of some of the above terminology).

With a harmonic point source of unit strength and angular frequency w, the velocity potential Φ (an indication of sound pressure) at any field point (r,θ,z) in the cylindrical coordinate system defined in figure 2.4 must satisfy the wave equation:

$$\nabla^2\phi + \left[\frac{w}{c(z)}\right]^2\phi = -\frac{1}{r}\delta(r)\delta(\theta)\delta(z-z_o) \quad \ldots\ldots \quad (2.1)$$

Through a separation-of-variables technique eq. (1) leads to the following general normal mode solution to the initial boundary value problem;

$$\phi(r,\zeta) = A \sum_{n=1}^{n} U_n(\zeta_o)U_n(\zeta)H_o^{(1)}(k_n r) \quad \ldots \quad (2.2)$$

where it is observed that $\phi(r,\zeta)$ is basically a summation of the product of two similar functions. These ($U_n(\zeta_o)$, $U_n(\zeta)$) are the N discrete normal modes or eigenfunctions, evaluated at the normalised source and receiver depths respectively ($\zeta_o = z_o/H_1$; $\zeta = z/H_1$). $H_o^{(1)}(k_n r)$ is the Hankel solution in range with k_n the complex (due to attenuation) wave number or eigenvalue.

In summary them, as described in section 2.2, the normal mode approach involves expanding the solution to the wave equation in terms of normal modes in the vertical (pressure vs depth distribution,($U_n(\zeta)$) and cylindrically spreading waves in the horizontal ($H_o^{(1)}$ $(k_n r)$).

2.4 Transmission loss

As sound moves away from the source its intensity will generally decrease due to physical spreading. Due to the refractive nature of the variable sound velocity structure, bending of sound *rays* will occur and areas of higher and lower sound intensity will occur (e.g. the SOFAR channel vs a shadow zone). Reflections from the sea surface and bottom can also contribute to specific sound intensity distributions in range away from the source.

While the loss in sound intensity described so far can be attributed to the geometry and physical nature of the oceanic environment, other loss mechanisms due to mechanical and chemical effects also contribute towards the overall sound propagation or transmission loss. These losses tend to be strongest at higher frequencies so that the net result is that low frequency sound has the potential of further overall propagation range - a major factor in support of low frequency sound propagation research.

Normal mode theory can be used effectively in calculating transmission loss since all the necessary physics are included to account for all the loss mechanisms described above. Signal field attenuation is introduced by allowing the wave number (k_n) of each mode to become complex ($k_n \rightarrow k_n + i\ \delta_n$). This attenuation coefficient can be seen in equations 2.3 and 2.4 below while a breakdown of it into separate loss mechanisms is performed in section 3.5.

When the phases of the individual modal pressure contributions are included in the summation, coherent transmission loss is calculated:

$$TL_c = -10 \log \left[\frac{(2\pi\rho_1^2)}{H_1^2} \left\{ \left(\sum_{n=1}^{N} \frac{U_n(\zeta_o)U_n(\zeta)}{(k_n r)^{1/2}} e^{-\delta_n r} \cos(k_n r) \right)^2 + \left(\sum_{n=1}^{N} \frac{U_n(\zeta_o)U_n(\zeta)}{(k_n r)^{1/2}} e^{-\delta_n r} \sin(k_n r) \right)^2 \right\} \right] \quad . \quad (2.3)$$

When the energy contributions of individual modes rather than the phased pressures are added, incoherent transmission loss is calculated:

$$TL_i = -10 \log \sum_{n=1}^{N} \left[\frac{(2\pi\rho_1^2)}{H_1^2} \sum_{n=1}^{N} \left\{ \frac{U_n(\zeta_o)U_n(\zeta)}{(k_n r)^{1/2}} e^{-\delta_n r} \right\}^2 \right] \quad \ldots\ldots\ldots\ldots\ldots\ldots\ldots\ldots \quad (2.4)$$

Phase interference effects in the coherent summation lead to oscillations in the typical transmission loss curve in figure 2.5. Similar oscillations are indeed exhibited by many sound propagation measurements employing continuous wave (CW) acoustic signals. However, in a typical measurement scenario, detail of many of the environment parameters (sound velocity profiles, exact bottom composition etc.) is not known with sufficient accuracy to permit exact agreement between calculated and measured interference patterns. For this reason, the incoherent result in figure 2.5 is often used to consolidate the model versus measurement problems.

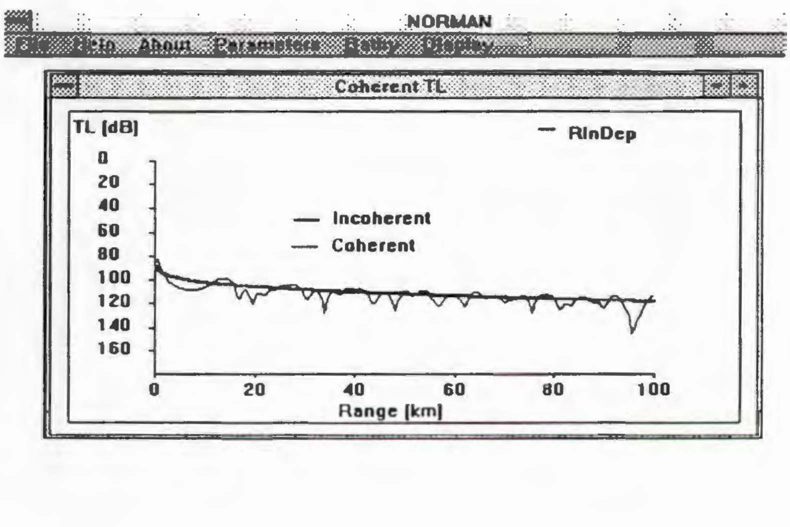

Figure 2.5: Typical coherently and incoherently calculated transmission loss ([10]).

2.5 Conclusions

Underlining the intrinsic potential of model NORMAN, a few features of the normal mode approach according to a model analysis by Jensen ([5]):

- Normal mode theory has been well-formulated and documented and is the most popular wave-theoretic modelling tool for range-independent low frequency sound propagation in shallow water.

- The complete normal mode solution can be highly automated for computer implementation.

- Excellent agreement also exist between normal mode predictions and sound propagation measurements.

- Frequency cut-off in shallow water and surface ducts is well-explained through the normal mode approach.

- The normal mode procedure can also easily be extended to slightly range-dependent environments through the adiabatic approximation.

CHAPTER 3: MODEL NORMAN

3.1 Introduction

NORMAN was written and is still being further developed by MP Stander at the Institute for Maritime Technology. While the mode and sound propagation loss solution technique is very similar to that of Miller and Ingenito ([1]), all further output options and result formats are the result of independent and original work as far as selection, presentation and specific solution techniques are concerned. User friendliness, in- and output flexibility as well as seizing the multiple output format inherent to a Windows environment, were the main goals in creating the software.

With the underlying theory of normal modes described in the previous chapter, detail of the locally developed normal mode sound propagation model, NORMAN, can now follow.

3.2 Program input

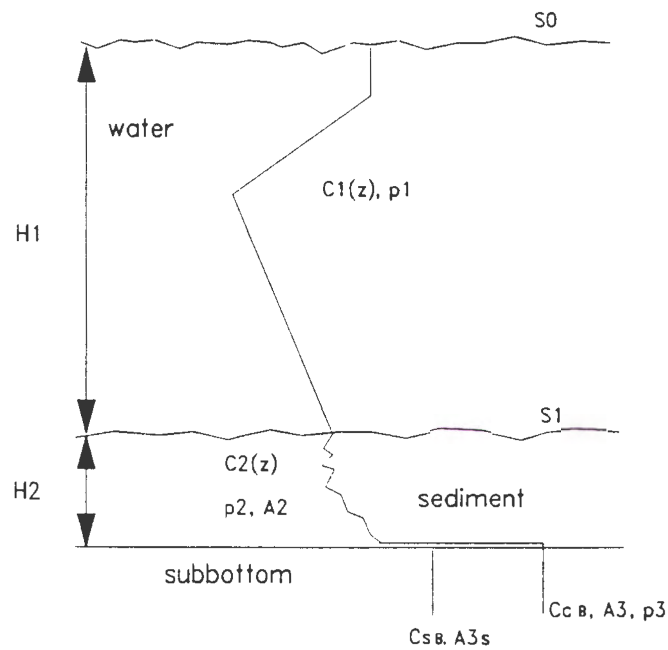

Figure 3.1: NORMAN environment.

Consistent with the physical model and definitions in figure 2.4, a similar input environment holds for NORMAN. When a definite hard sub-bottom supporting shear waves is present, a "SOLID" solution is calculated, while a "FLUID" solution is performed when the sub-bottom is replaced by a second sediment layer which does not support shear waves.

When two distinct bottom layers with different properties are not required, a two-layer model can be realised by giving the sediment layer a small thickness and physical properties identical to those of either the water layer (SOLID or FLUID) or of the basement (FLUID only).

Input parameters to NORMAN can be seen in table 3.1.

TABLE 3.1:

PARAMETER AND EXPLANATION	SYMBOL	UNIT
MODEL (SOLID or FLUID-version)	-	-
Sound velocity profile (depth, sound speed table)	SVP	-
Frequency	F	Hz
First layer depth (water depth)	H_1	m
Second layer depth (sediment or water depth)	H_2	m
Compressional sound speed in basement or sediment	c_{CB}	m/s
Shear sound speed in basement	c_{SB}	m/s
Source depth	z_o	m
Receiver depth	z	m
TL-window start point in range	r_{min}	m
TL maximum calculation range	r_{max}	m
TL analysis range increment	incr	m
Water density	ρ_1	g/cm^3
Water or sediment density	ρ_2	g/cm^3
Sediment or basement density	ρ_3	g/cm^3
Number of incremental layers in water	NL_1	-
Number of incremental layers in water or sediment	NL_2	-
Lowest mode-number to calculate	LM	-
Highest mode-number to calculate	HM	-
Surface rms roughness	S0	m
Bottom rms roughness	S1	m
Compressional absorption coefficient in sediment	A_2	dB/Hz.m
Compressional absorption coefficient in basement	A_3	dB/Hz.m
Shear absorption coefficient in basement	A_{3S}	dB/Hz.m

3.3 Program output

NORMAN can generate the following results: (Although some output examples share common input data as will be indicated, an analysis of a specific input set is not intended).

3.3.1 Sound velocity profile (SVP) graphics

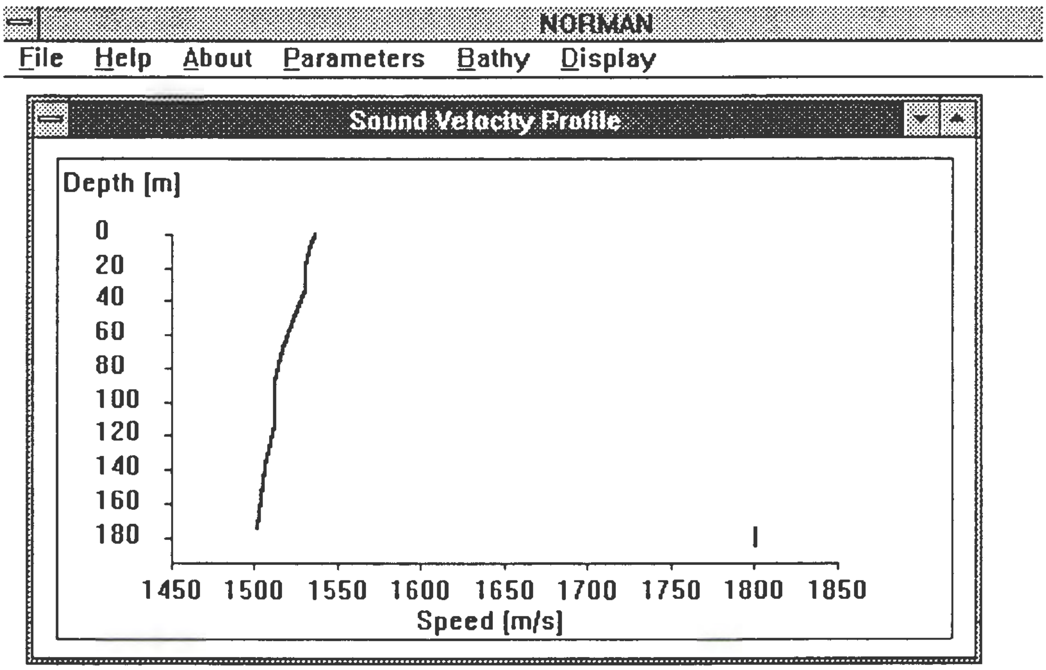

Figure 3.2: Sound velocity profile (Durban, summer).

3.3.2 Normal mode or eigenfunction graphics

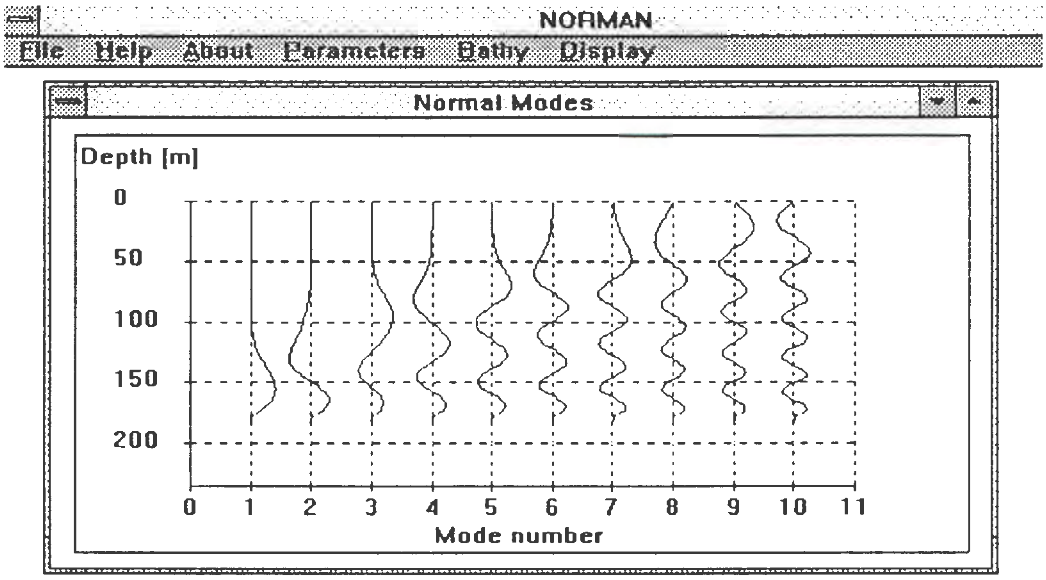

Figure 3.3: The normal modes for the SVP in figure 3.2.

3.3.3 Coherent and incoherent TL vs Range plots for a range-independent environment

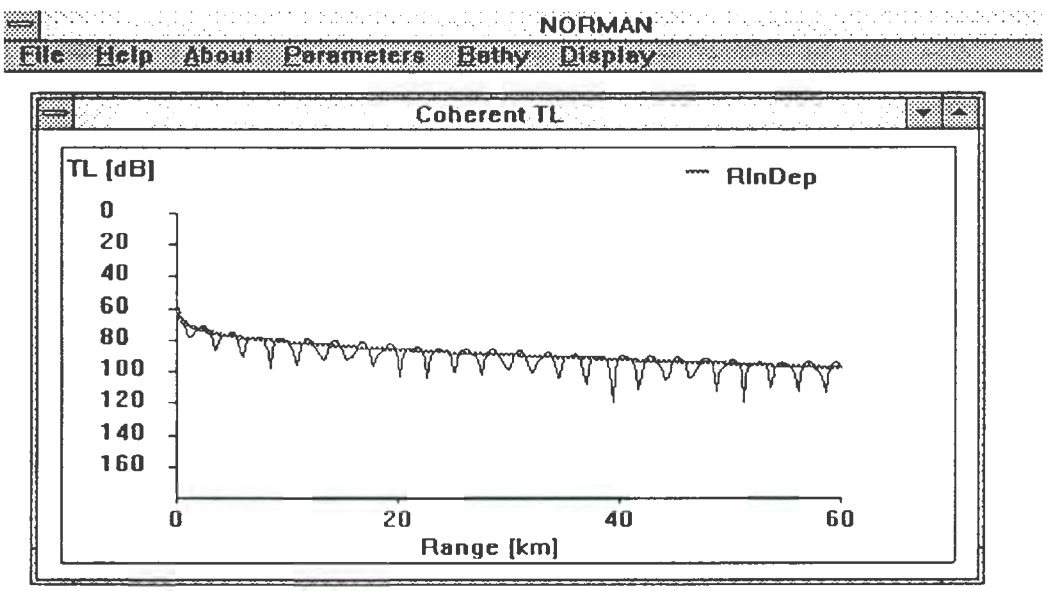

Figure 3.4: Transmission loss vs range.

It is important to realise that the source and receiver depths are included in the above transmission loss calculations so that the result uniquely specifies the loss from the source to the receiver. In a ray-theory analogy it implies that transmission loss is only calculated along the eigen-rays.

3.3.4 Coherent and incoherent TL vs Range plots for a range-dependent environment

The range-dependent capability will be illustrated in chapter 4.

3.3.5 Acoustic field map for a range-independent environment

The specific result capability, similar to a ray diagram adds a visual presentation of sound intensity distribution.

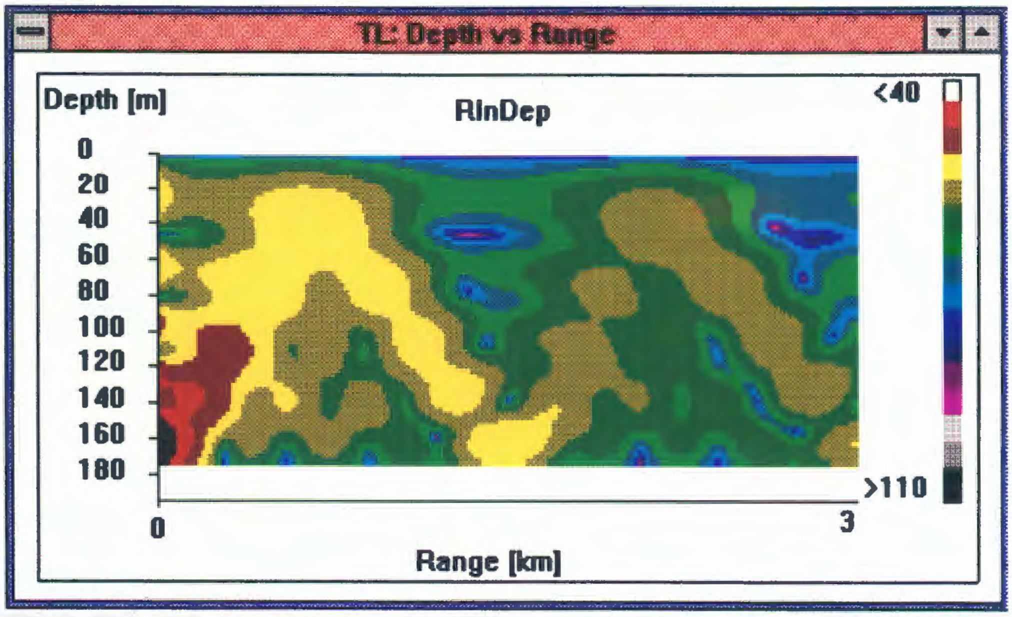

Figure 3.5: Transmission loss: Depth vs Range acoustic field map.

3.3.6 Optimum frequency calculation

An optimum frequency with regards to minimum transmission loss versus range for a specific environment with specific source and receiver depths, can be calculated.

A more thorough explanation as well as examples can be seen in section 4.4.

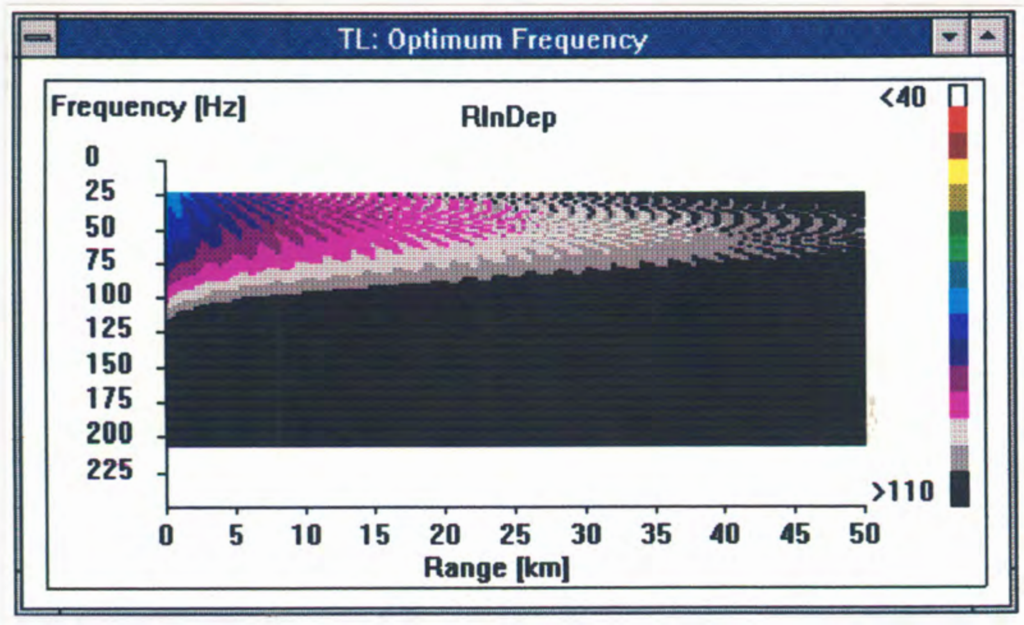

Figure 3.6: Optimum frequency calculation (50 Hz).

3.3.7 Listed calculation results

- Modal wave numbers or eigenvalues.
- Individual modal propagation loss.
- Mode velocities.

3.4 Program composition and execution

NORMAN is written and compiled in *Turbo Pascal for Windows* (version 1.5) in the following main Units:

NOR_WIN	main program
GLOBVAR	contains global variables
DETMODE	calculates eigenfunction
INTERVAL	determines eigenvalues through interval reduction
MMAT	contains various shared mathematical procedures
PLOSS	calculates transmission loss
NORMHELP	contains help information
VALIDIZE	checks for valid parameter input

The executable version, NORMAN version 2, runs in a *Windows* environment, incorporates pull-down menus for input listing and output selection and can produce a multiple result screen as can be seen in figure 3.7.

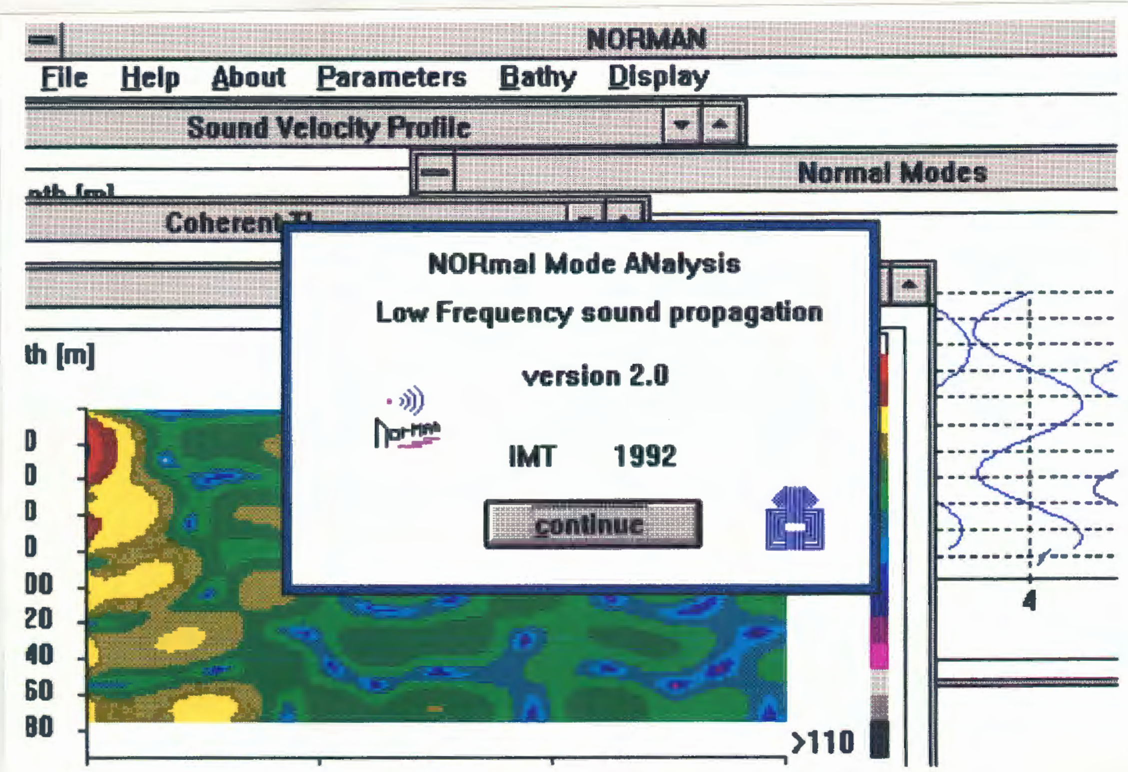

Figure 3.7: Multiple results (windows) displayed by NORMAN.

The basic normal mode computer code is based on a study of the solution described by Miller and Ingenito ([1]).

3.5 Transmission loss calculation

Since TL is the most important output generated by NORMAN, it is important to investigate the separate loss mechanisms incorporated by the model.

In equations 2.3 and 2.4 an attenuation coefficient was introduced because the modal wave numbers became complex in nature. This is the result of the following physical mechanisms ([1]):

$$\delta_n = \sum_{i=1}^{6} loss\ (i) \qquad (3.1)$$

where

loss (1)	=	$\epsilon_2\ \gamma_n^{(2)}$	:	sediment plane-wave compressional attenuation
loss (2)	=	$\epsilon_{3c}\ \gamma_n^{(3c)}$	:	basement plane-wave compressional attenuation
loss (3)	=	$\epsilon_{3s}\ \gamma_n^{(3s)}$	:	basement plane-wave shear attenuation
loss (4)	=	$S0,n$	:	surface reflection loss
loss (5)	=	$S1,n$	:	bottom reflection loss
loss (6)	=	α_n	:	water absorption . . . . (3.2)

where ϵ_2 and ϵ_{3c} are the plane-wave attenuation coefficients of the material in the sediment and basement respectively. ϵ_{3s} represent the shear plane-wave attenuation coefficient of the basement, while the quantities $\gamma_n^{(2)}$, $\gamma_n^{(3c)}$ and $\gamma_n^{(3s)}$ measure the degree to which the nth mode interacts with the sediment and basement compressional and shear wave mechanisms. *S0,n* and *S1,n* represent acoustic field attenuation due to modal interaction with statistically rough boundaries at the water surface and the water-sediment boundary, respectively.

3.6 Benchmarking

With reference to chapter 1 regarding the accuracy of existing sound propagation models, it seems logical to use such model output as a measure of the accuracy and efficiency of program NORMAN.

3.6.1 Test case 1

This first test case from reference [4] is widely published and is aimed at determining model accuracy since the TL-curve has much detail due to modal interference. The source and receiver are just off the bottom and therefore cause the higher order modes to be more strongly exited. This results in a wide vertical beam width (37°) which provides the ideal benchmark for a PE-model which is inherently a narrow angle tool. Normal mode models handle wide vertical angles well and therefore usually supply the benchmarks for the PE-models. NORMAN can therefore in turn, be measured against such a normal mode model, in this case SNAP ([3]). The model input parameters appear in Table 3.2.

This benchmark is also documented in reference [6], where a PE-model (GRAPES, 1990) is benchmarked against the normal mode model, SNAP ([3]).

TABLE 3.2:

PARAMETER	VALUE	UNIT
MODEL	FLUID	-
Sound speed in water (isovelocity)	1 500	m/s
F	250	Hz
H_1	100	m
H_2	10	m
c_{CB}	1 590	m/s
zo, z	99.5	m
r_{min}	5 000	m
r_{max}	10 000	m
incr	4	m
ρ_1	1	g/cm^3
ρ_2, ρ_3	1.2	g/cm^3
NL_1	60	-
NL_2	40	-
LM	1	-
HM	11	-
A_2, A_3	0.00031	dB/Hz.m
Other parameters	0	-

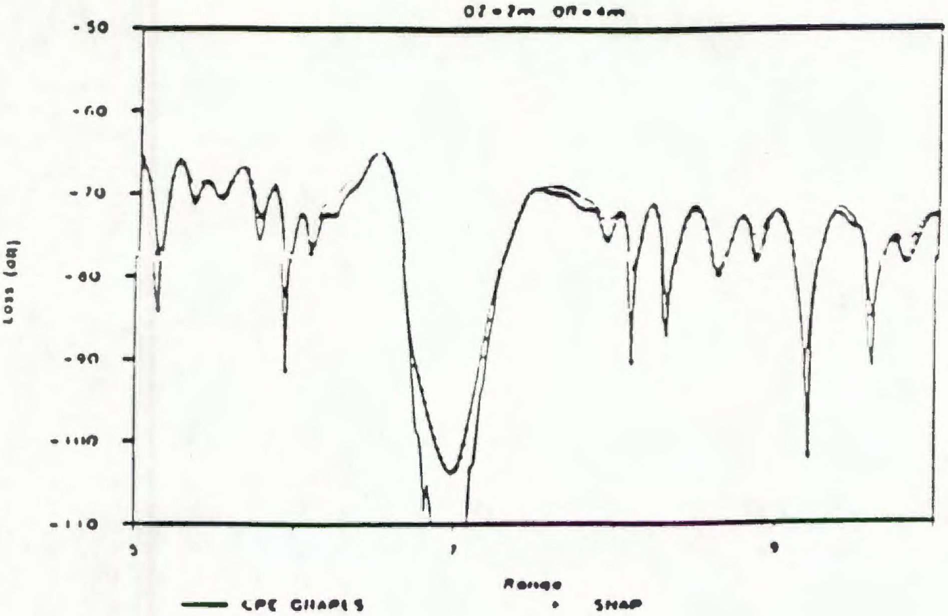

Figure 3.8: GRAPES vs SNAP ([6]).

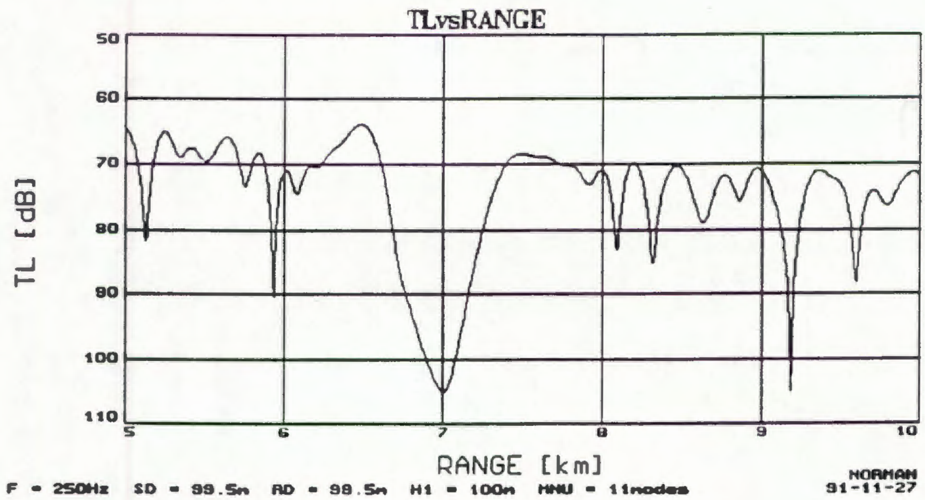

Figure 3.9: NORMAN Transmission loss prediction.

From figures 3.8 and 3.9 it is clear that NORMAN matches the SNAP prediction very closely, in fact more accurately than GRAPES. Since SNAP is not locally available, it is not possible to directly compare accuracy and computational time. Reference [6] reports a computation time of 29 minutes for GRAPES for this calculation. In comparison

NORMAN's time is less than 1 minute on a 486 IBM PC.

3.6.2 Test case 2

Finally, for identical input, three other model TL-outputs are compared to NORMAN, i.e. SNAP (Normal Mode), PAREQ and IFD (both PE). (Test case source: reference [4].) See appendix A for more detail of the foreign models.

TABLE 3.3:

PARAMETER	VALUE	UNIT
MODEL	FLUID	-
Sound speed in water (isovelocity)	1 500	m/s
F	500	Hz
H_1	100	m
H_2	20	m
c_{CB}	1 550	m/s
zo, z	50	m
r_{min}	0	m
r_{max}	25 000	m
incr	25	m
ρ_1	1	g/cm^3
ρ_2, ρ_3	1.2	g/cm^3
NL_1	100	-
NL_2	40	-
LM	1	-
HM	17	-
A_2, A_3	0.00065	dB/Hz.m
Other parameters	0	-

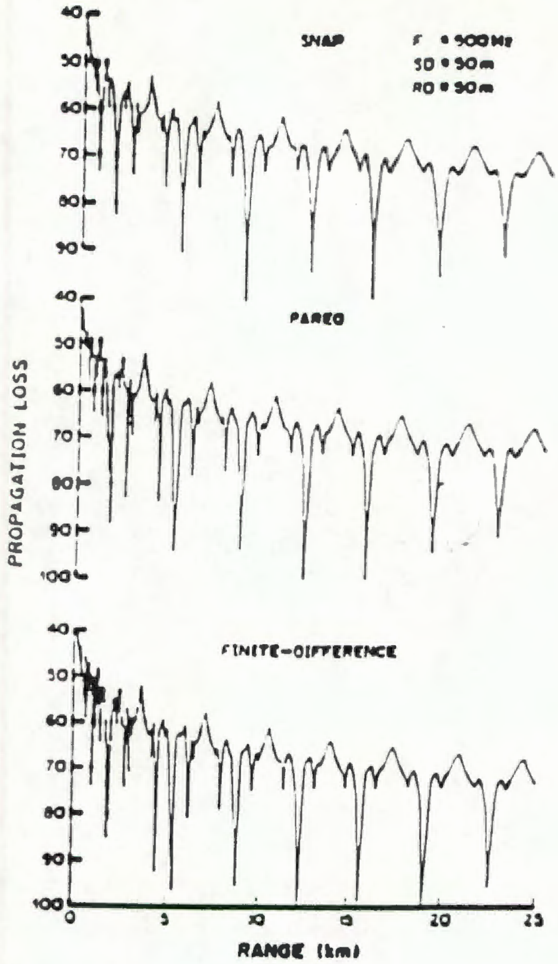

Figure 3.10: SNAP, PAREQ and IFD Transmission loss ([4]).

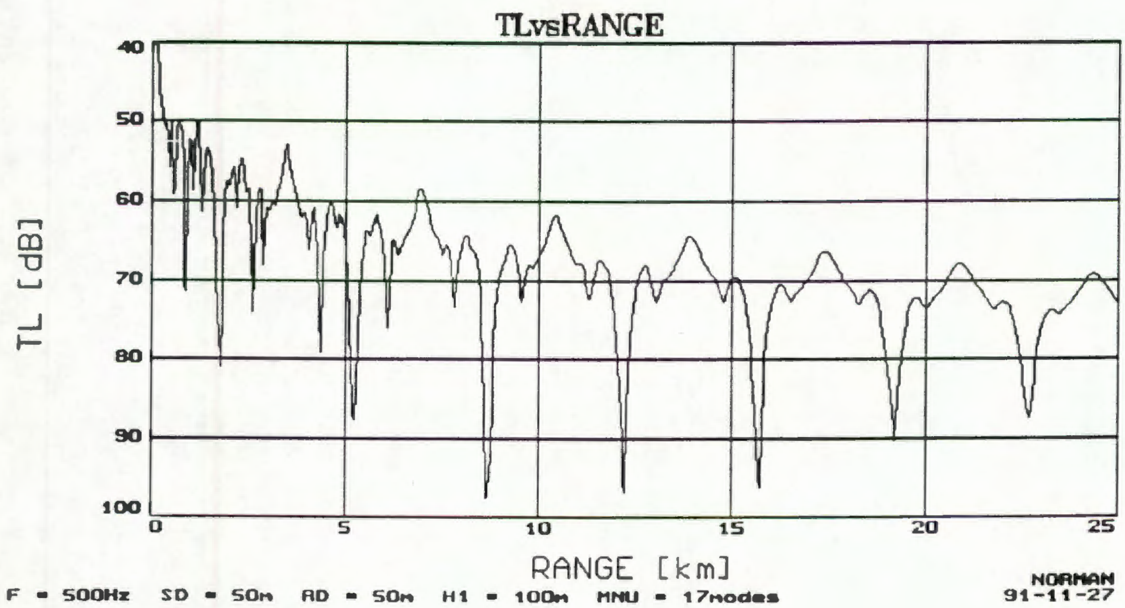

Figure 3.11: NORMAN Transmission loss prediction.

The excellent agreement is obvious from figures 3.10 and 3.11.

3.7 Conclusions

Apart from reporting the model structure and capability, it has been illustrated in this chapter that normal mode theory as described in chapter 2 is practically applied by model NORMAN in producing sound propagation prediction results that, in the local context, were not possible before.

CHAPTER 4: NORMAL MODE APPLICATION

4.1 Introduction

The following subjects are treated from a normal mode wave theory point of view in this chapter:

- Range-dependent sound propagation loss
- Ducted sound propagation
    - Surface ducts
    - Deep sound channel
- Optimum frequency analysis
- Sonar application
- Sound propagation experiments

Sound propagation loss in a range-dependent environment is specifically included because the need to address this topic is central to the original requirement stated in chapter 1. Ducted sound propagation implies cylindrical sound spreading which is theoretically well-accounted for by the normal mode approach. The deep sound channel is also extensively used for remote sensing. A prime example of this is the current Global Warming programme in which South Africa is a keen participant. Both the optimum frequency analysis and the sonar application sections are examples of how basic model output can be extended and applied in order to provide useful and practical information. Always important to a modelling is a validation phase and this was, apart from benchmarking (chapter 3), achieved by sound propagation experiments at sea.

While many if not all of these applications are valid study fields on their own, they are grouped together to provide a greater understanding of normal mode theory, as well as the creation of a local awareness regarding the usefulness and application of a sound propagation model based on such theory.

4.2 Transmission loss in a range-dependent environment

4.2.1 Introduction

Transmission loss in a range-independent environment has been treated in sections 2.4 and 3.5 and examples of NORMAN TL calculations have been shown. The aim of this section is to demonstrate how normal mode theory can be applied in order to perform transmission loss calculations in a range-dependent environment.

Even over relatively short propagation paths (less than 10 km) the geometry and acoustical properties of the medium do depend upon range. When such an environment is now introduced, the previous technique for solving the wave equation (separation-of-variables) is not valid any more and it therefore becomes necessary to employ approximation techniques.

4.2.2 Approximations

In the first approximation it is assumed that the range-dependence is sufficiently slow for the wave equation to be locally separable. This implies that in the vicinity of some point in the range-dependent medium, any property of a specific normal mode is the same as it would be in a hypothetical range-independent medium with an environment identical to the point of interest. This "local" environment can then be used to calculate local properties from the range-independent model. From these local properties intermediate properties are then calculated by means of linear inter- or extrapolation.

The second approximation, called the adiabatic approximation or the conservation of mode index, states that the range-dependent environment does not transfer energy from one mode to another.

When these two approximations are now applied to the transmission loss equations (2.3 and 2.4), the following modifications are necessary: (The unprimed quantities(U_n, H_1) apply to the source location and the primed ones (U'_n, H'_1) to the field point at range r.)

$$U_n(\zeta_o)U_n(\zeta) \quad \rightarrow \quad U_n(\zeta_o)U'_n(\zeta) \qquad (4.1)$$

$$H_1 \quad \rightarrow \quad \sqrt{H_1 H'_1} \qquad (4.2)$$

A *cumulative* phase and an *average* attenuation coefficient must also now be introduced:

$$k_n r \quad \rightarrow \quad \varnothing_n \equiv \int_o^r k_n(r)dr \qquad (4.3)$$

$$\delta_n \quad \rightarrow \quad \Delta_n \equiv \frac{1}{r}\int_o^r \delta_n(r)dr \qquad (4.4)$$

Coherent and incoherent transmission is therefore now calculated in the following manner([2]):

$$TL_c = -10 \log\left[\frac{(2\pi\rho_1^2)}{H_1 H_1'}\left\{\left(\sum_{n=1}^{N}\frac{U_n(\zeta_o)U_n'(\zeta)}{(\varnothing_n)^{½}}\,e^{\Delta_n r}\cos(\varnothing_n)\right)^2 + \left(\sum_{n=1}^{N}\frac{U_n(\zeta_o)U_n'(\zeta)}{(\varnothing_n)^{½}}e^{-\Delta_n r}\sin(\varnothing_n)\right)^2\right\}\right] \qquad (4.5)$$

$$TL_i = -10 \log\left[\frac{(2\pi\rho_1^2)}{H_1 H_1'}\sum_{n=1}^{N}\left\{\frac{U_n(\zeta_o)U_n'(\zeta)}{(\varnothing_n)^{½}}\,e^{-\Delta_n r}\right\}^2\right] \qquad (4.6)$$

4.2.3 Range-dependent application

The approximations described above were successfully incorporated into NORMAN, thereby giving the model a range-dependent capability. To demonstrate this, test case 1 in section 3.6.1 will serve as model input at zero range. Another input set, identical to test case 1 except for the water depth now being 110 m (was 100 m), will be read in at a second input range of 8 km. Transmission loss calculated for the range-dependent (sloping bottom) input can be seen in figure 4.1.

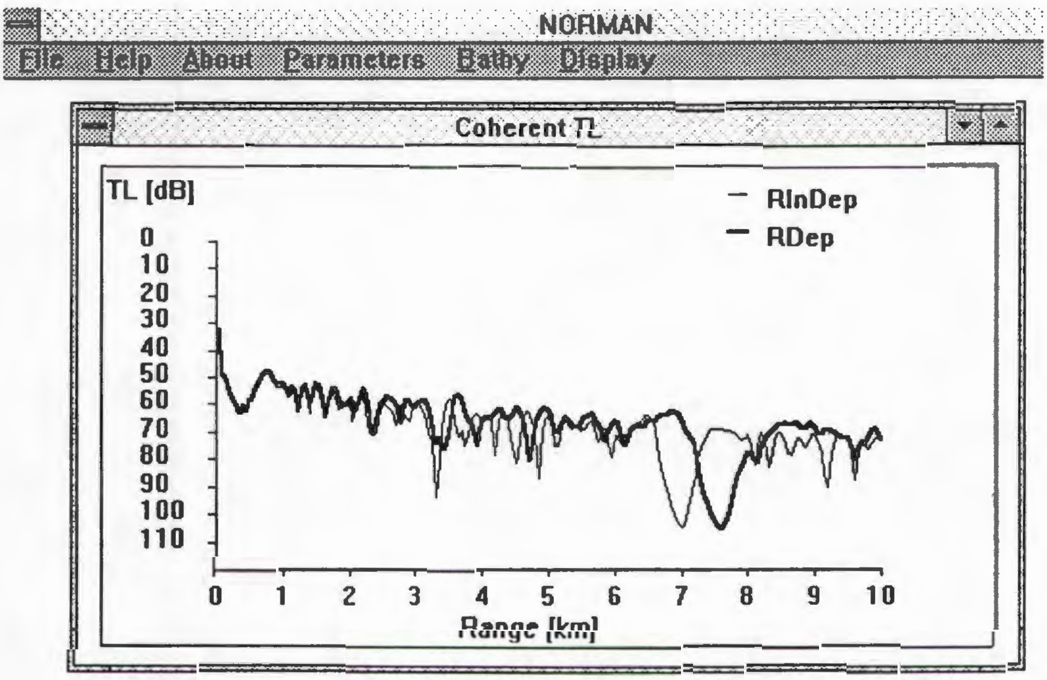

Figure 4.1: TL for a range-dependent environment calculated by NORMAN.

Note the almost 1 km shift of the characteristic transmission loss dip, due to the water depth increase of only 10 m over a 8 km increase in range.

4.2.4 Conclusion

The importance of being able to incorporate range-dependency into a sound propagation model as well as to have accurate knowledge of the analysis environment is emphasized by the difference in transmission loss prediction in figure 4.1. In other words, a slight change in the model input might lead to a significant change in result.

Two input ranges can be handled by NORMAN at this stage, but it is recommended that this number be increased to at least five, in order to model more environment detail over longer sound propagation analysis ranges.

As stated, the approximations incorporated into model NORMAN are only valid for a "slow" range-dependency. For more abrupt environmental changes, mode-coupling can be considered. More information on this topic as well as more references are documented by McDaniel in reference ([7]).

Note that an additional input set may differ from another by any arbitrary combination of the environmental parameters, but the fluid-basement and the solid-basement models may not be both used along the same analysis range.

4.3 Ducted sound propagation

4.3.1 Surface duct sound propagation

4.3.1.1 Introduction

An isothermal layer near the ocean surface is often created and maintained by wind mixing. A positive sound velocity gradient is then formed due to the pressure-depth effect. Such a SVP can be seen in figure 4.2.

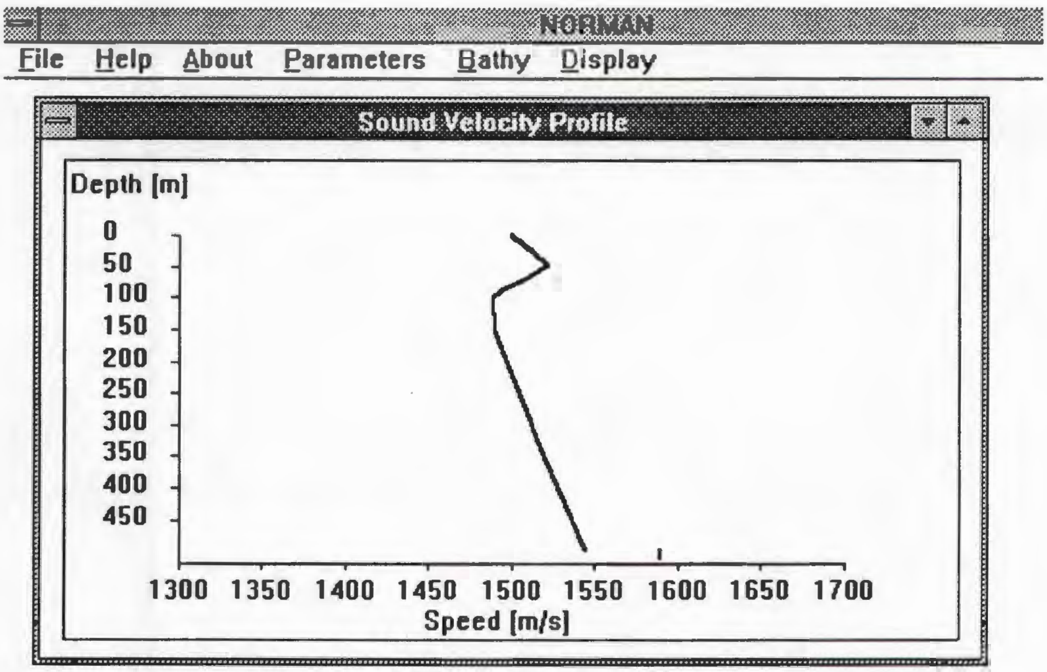

Figure 4.2: Typical surface duct sound velocity profile.

Should an acoustic source now be placed in this mixed layer, a cone of rays will be trapped in the layer due to the upward refraction, and a sound propagation duct will therefore be formed.

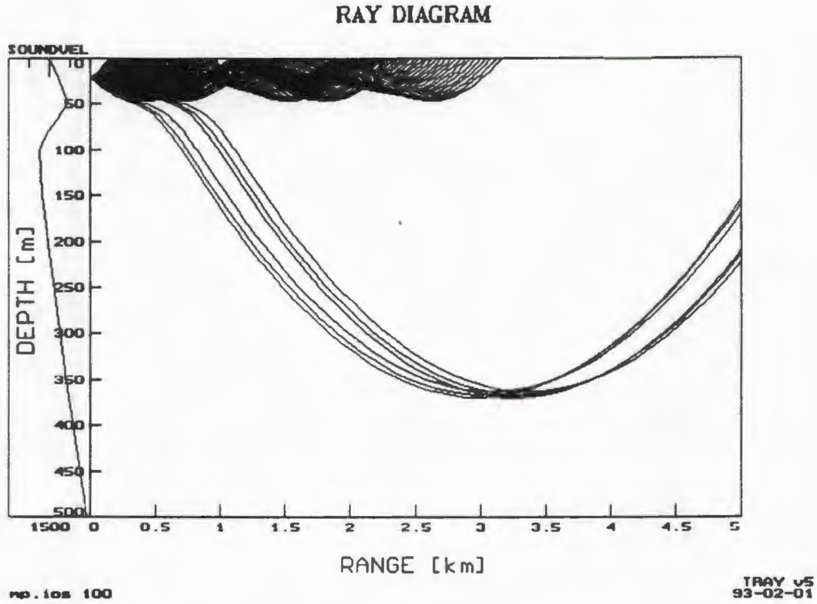

Figure 4.3: Surface duct sound propagation ([20]).

From figure 4.3 it can be expected that sound trapped in a surface duct can be received by a distant receiver, also in the duct. The efficiency of such a propagation path is a function of mixed layer depth, the positive sound velocity gradient as well as the source frequency. It will now be shown how a normal mode analysis can be most informative when the cut-off frequency for a surface duct sound propagation path must be determined.

4.3.1.2 Normal mode analysis and cut-off frequency

Based on amongst others the radar theory of ground-based ducts, empirical formulae for determining cut-off frequency are often used. However, such an approach is often an over simplification which does not take the prevailing sound propagation conditions and environment into account.

When a sound source (200 Hz) is now deployed at 20 m within the mixed layer for the profile in figure 4.2, the normal modes shown in figure 4.4 are calculated with NORMAN.

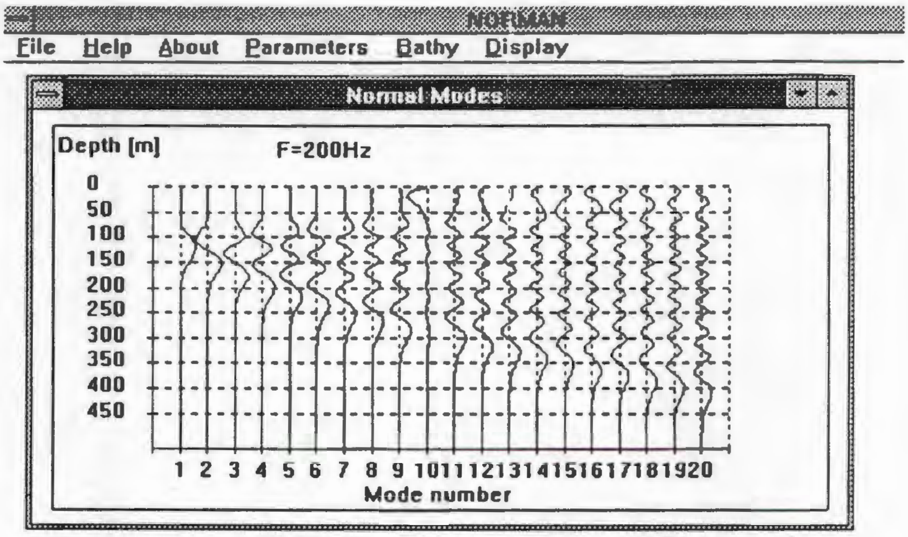

Figure 4.4: Normal modes for the profile in figure 4.2.

A summation of all these modes provide the coherent transmission loss shown in figure 4.5.

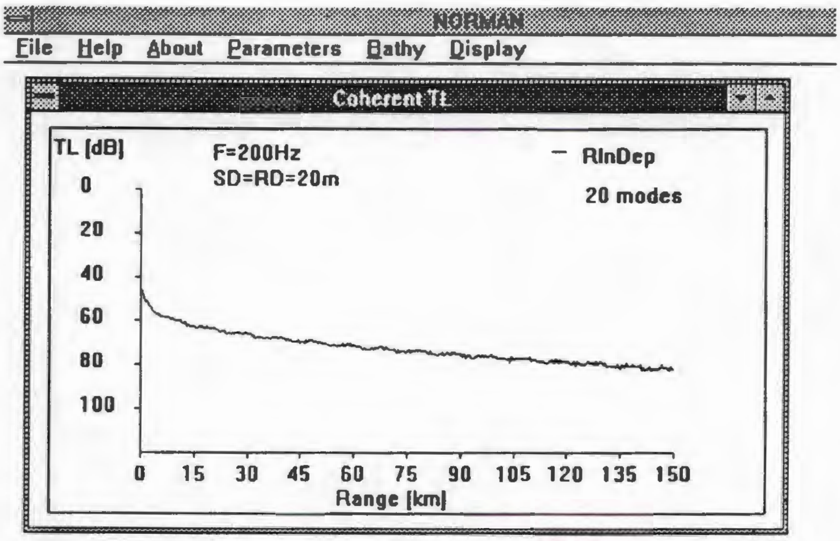

Figure 4.5: TL vs range (20 modes).

If the modes in figure 4.4 are now studied for individual contribution towards sound propagation within the surface duct, it should be quite obvious that mode 10 in particular, will be a dominant contributor. In fact, if the TL result from the first 8 modes (figure 4.6) is compared to the results for only modes 9 to 12 (figure 4.7), it can be seen that the latter summation almost solely contributes to the overall TL result in figure 4.5. It can therefore be expected that the absence of such a dominant mode (a *virtual* first mode according to Boyles in reference [15]) or modes can serve as a cut-off measure for surface duct sound propagation.

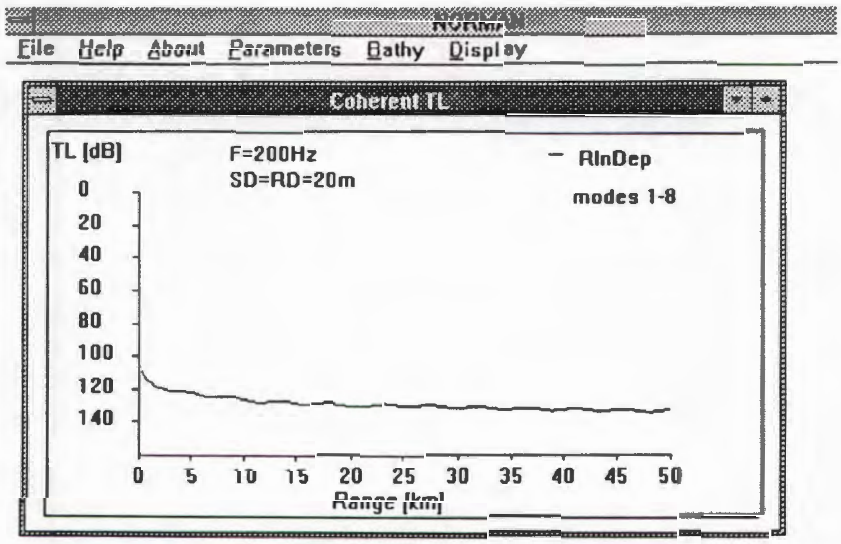

Figure 4.6: TL vs range (modes 1-8).

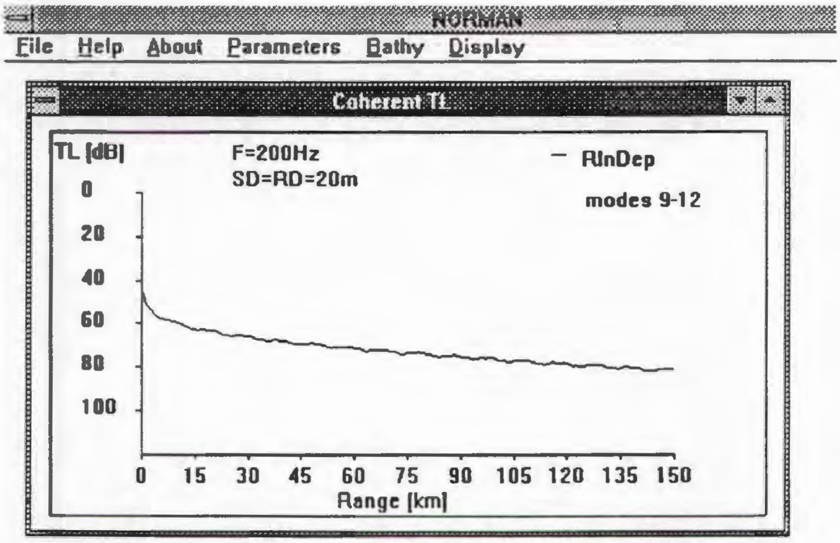

Figure 4.7: TL vs range (modes 9-12).

As was stated in section 2.2, each mode has a distinctive propagation velocity which lies between the SVP-minimum and maximum, and that a mode is activated by a source at the corresponding depth related to the specific mode velocity. The total number of modes is also a function of frequency, so that a higher frequency will support more trapped modes, while the reverse is true for a lower frequency.

How is this knowledge now applied to surface duct cut-off frequency and how can NORMAN be used to determine this frequency?

Should the source frequency be decreased from the 200 Hz case above, less overall modes will be trapped, as well as therefore fewer ones with propagation velocities between the surface velocity value and the maximum velocity in the mixed layer. The conditions for the formation of a dominant or virtual mode or a series of definite energy carrying modes therefore deteriorate until no such modes are eventually supported by the system. This is illustrated by figures 4.8 and 4.9 where very much higher transmission loss is predicted for a frequency of 25 Hz (only 5 modes in total) because no prominent surface duct modes are evident in figure 4.8. The rest of the original system remained the same.

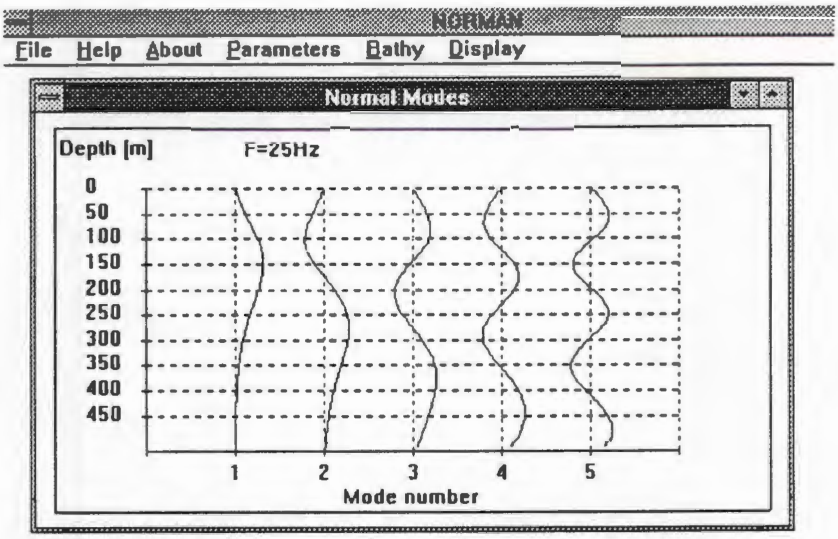

Figure 4.8: Normal modes at 25 Hz.

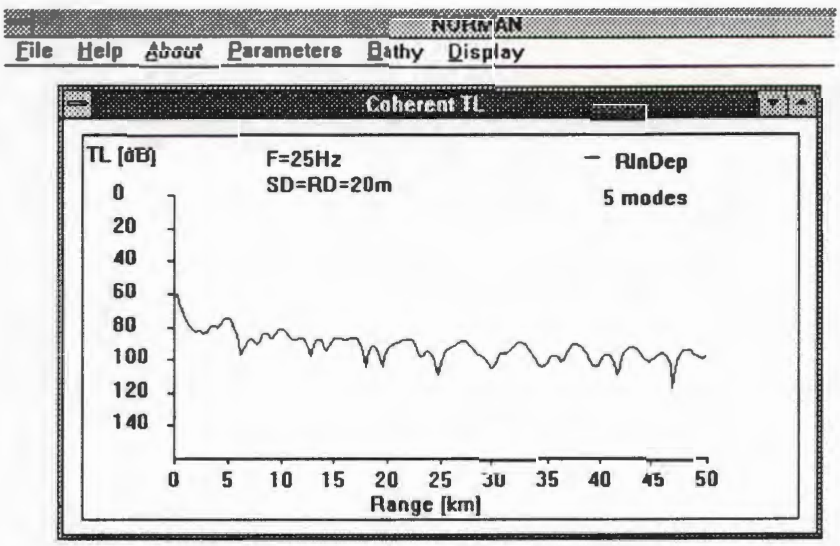

Figure 4.9: TL vs range (5 modes in total at 25 Hz).

4.3.1.3 Conclusion

Surface duct cut-off frequency can be explained and predicted by a normal mode analysis. It is also important to realise that the entire system (environment, frequency, source/receiver depths) affects the cut-off frequency.

Another important feature of normal mode theory was also unobtrusively utilised in this section. From figure 4.3, the ray diagram of the specific surface duct profile incorrectly predicts that a ll the energy trapped in the duct will remain there as the sound propagates down the duct. This implies that if transmission loss is calculated with such a ray theory model, the loss will be over-predicted below, and under-predicted within the duct. Normal mode theory on the other hand inherently incorporates diffraction leakage out of a surface duct as can be seen from figure 4.10, where a definite acoustic field is predicted below the well-defined surface duct.

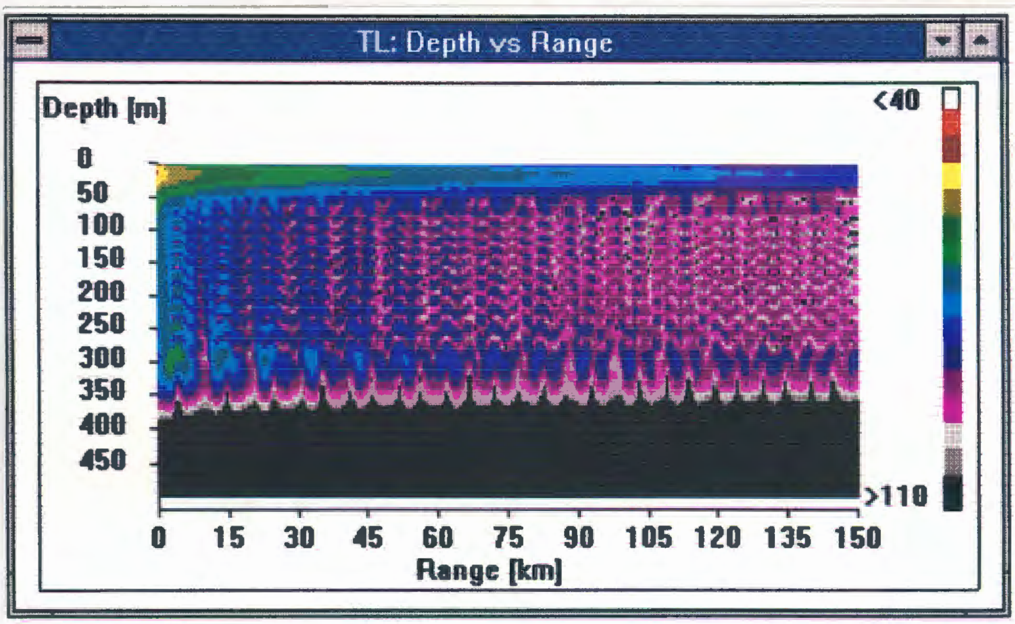

Figure 4.10: Transmission loss: Depth vs Range acoustic field map of a surface duct.

4.3.2 Deep sound channel sound propagation

4.3.2.1 Introduction

The deep sound channel or SOFAR-channel (SOund Fixing And Ranging) has significant relevance in long range sound propagation at low frequency because of the minimum propagation loss encountered.

Of specific current interest is the ATOC programme ([16]) whereby global warming is monitored by measuring ocean temperature changes as a function of acoustic travel times (in the SOFAR-channel) over very long ranges.

4.3.2.2 NORMAN and the SOFAR-channel

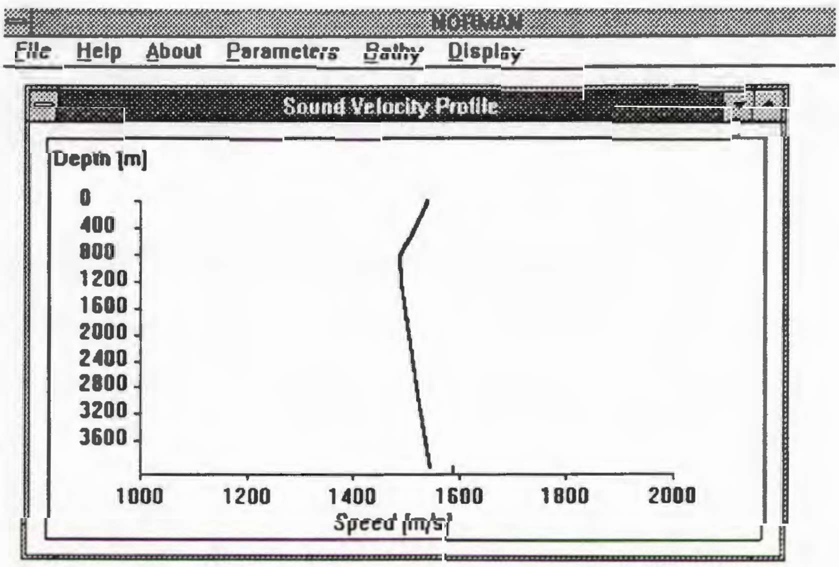

Figure 4.11: A deep water sound velocity profile.

For the typical deep water sound velocity profile in figure 4.11, the normal modes can be seen in figure 4.12.

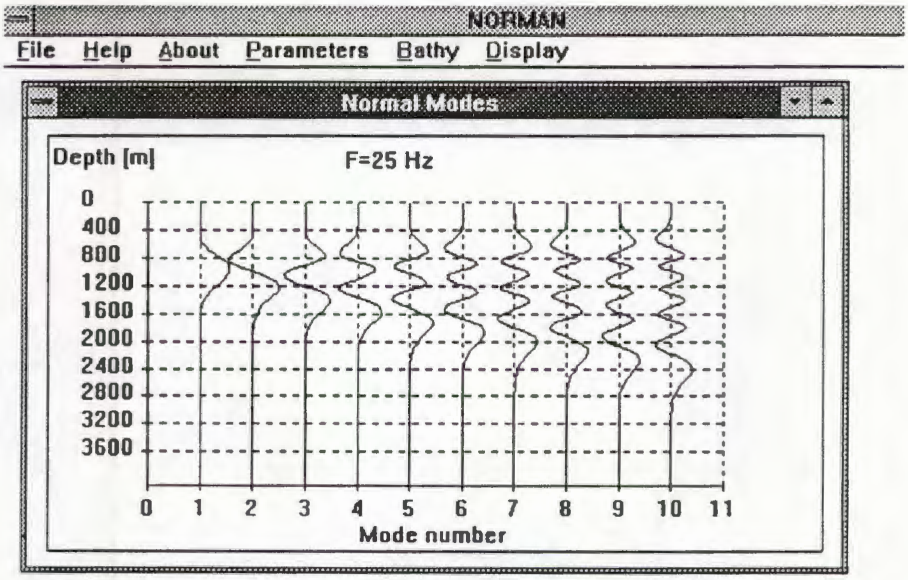

Figure 4.12: The normal modes for the SVP in figure 4.11.

It is expected that a transmission loss summation based on the first few modes will provide a relatively low TL vs range result over a long range in a range-independent scenario due to little or no surface or bottom interaction. This sound channelling effect can clearly be seen in figure 4.13.

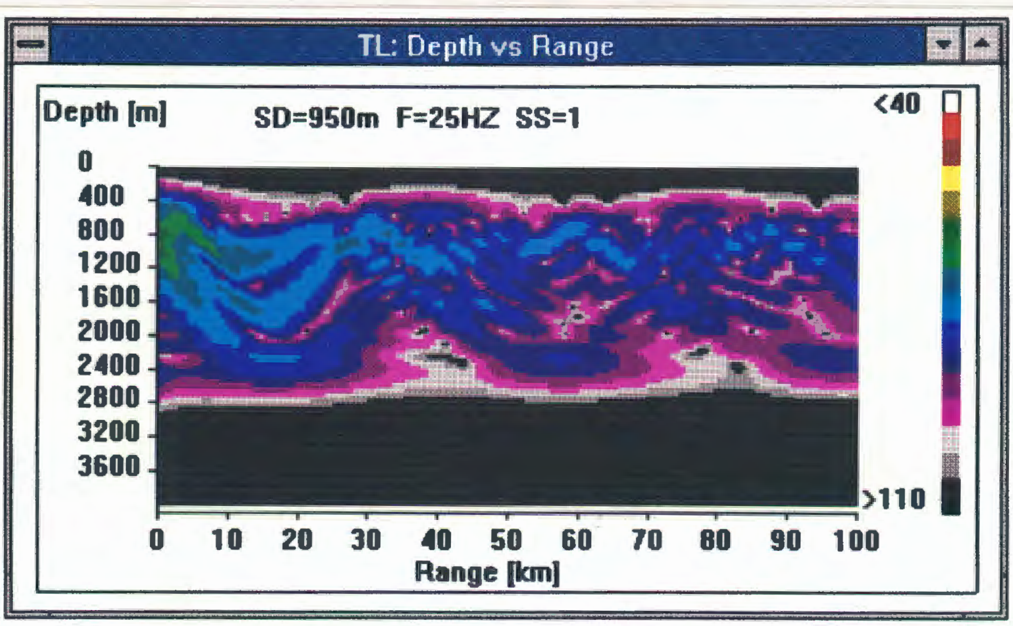

Figure 4.13: TL vs range in the SOFAR-channel.

4.3.2.3 SOFAR signal shape

In view of the current relevance of the ATOC programme, sound signal propagation in the deep sound channel will be further discussed.

The following theoretical mode behaviour is relevant:

- The first mode propagates with the lowest loss (small grazing angle) and at the lowest speed.

- The higher order modes propagate with higher loss and over a greater overall path length (higher grazing angles), as well as at higher speeds.

Should one now predict a time waveform arrival at a distant receiver (in the SOFAR-channel) due to a sound source also in the channel, the above mode theory can propose a signal shape according to the one in figure 4.14. Here the arrival pattern consists of a series of sharp pulses each identified with a given mode: the higher order modes arrive early, while the first mode comes in last (with maximum energy due to the least loss).

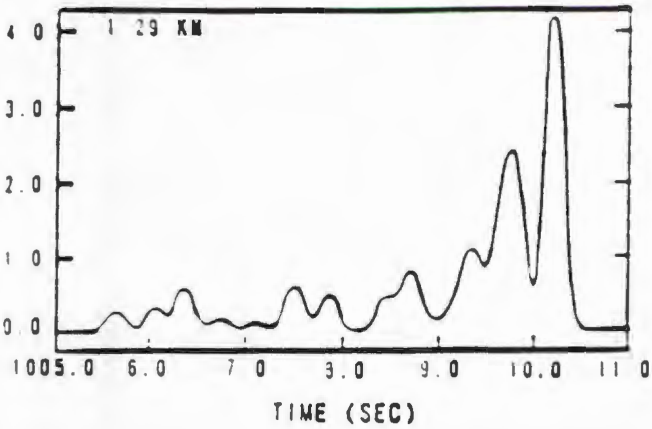

Figure 4.14: Predicted arrival pattern of SOFAR propagation ([17]).

As part of a feasibility test in optimising a sound source location near Cape Town (ATOC-FACT programme), explosive sound sources were deployed in the deep sound channel in November 1992. After a 4 200 km propagation path the signals were clearly received at Ascension by a number of hydrophones, each sampling a different water depth with respect to the minimum sound speed axis, as figure 4.15 indicates.

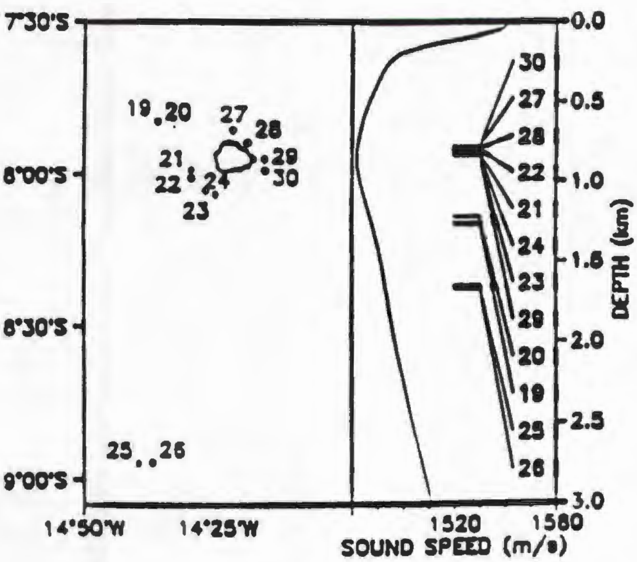

Figure 4.15: Hydrophone depths at Ascension.

If the time waveform arrival patterns for different shots at a specific hydrophone (no. 30) are now investigated, it can be seen from figure 4.16 that the signal structure for the shot 1 arrival at hydrophone 30 matches the predicted SOFAR arrival structure very well, while the shot 3 arrival clearly does not - most likely due to the source being off-axis.

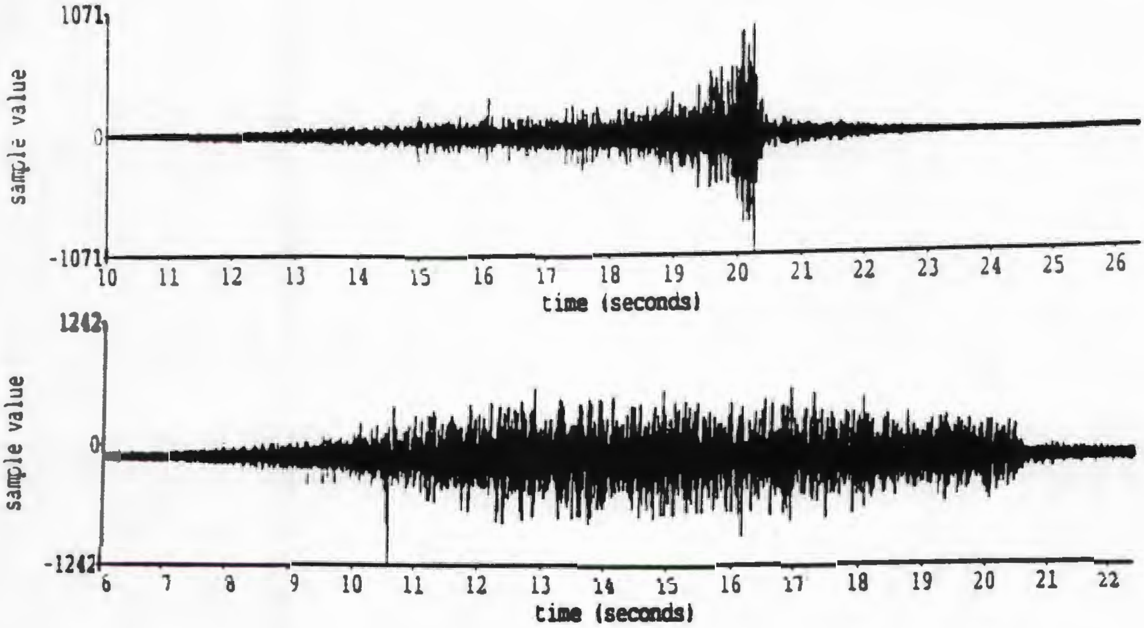

Figure 4.16: Arrival patterns of SOFAR signal shape at Ascension (shots 1 and 3).

4.3.2.4 Conclusion

While NORMAN currently can not determine arrival time and angle information, it has been shown that normal mode theory can be used to explain as well as predict SOFAR signal arrival structure.

It is also proposed that NORMAN should be extended in future as to include such an analysis capability.

4.4 Optimum frequency

4.4.1 Introduction

It is the aim of this section to, from a normal mode point of view, explain how an optimum frequency with regards to minimum sound propagation loss is established.

4.4.2 Optimum frequency calculation

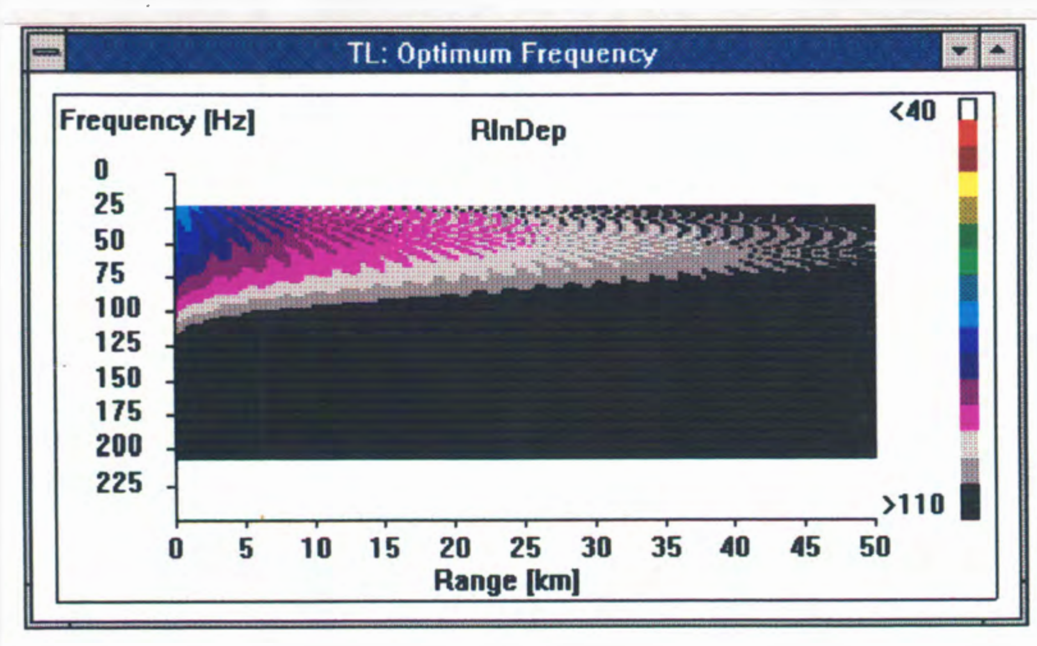

Figure 4.17: Optimum frequency calculation.

From figure 4.17 (a repeat of figure 3.6) it can be seen that minimum transmission loss with reference to range, for this specific example, is predicted at 50 Hz, and that this is visible as a peak along the frequency axis at 50 Hz.

This prediction is easily confirmed by looking at the two coherent transmission loss versus range graphs in figures 4.18 and 4.19, where the 50 Hz prediction is clearly much lower than the 200 Hz one.

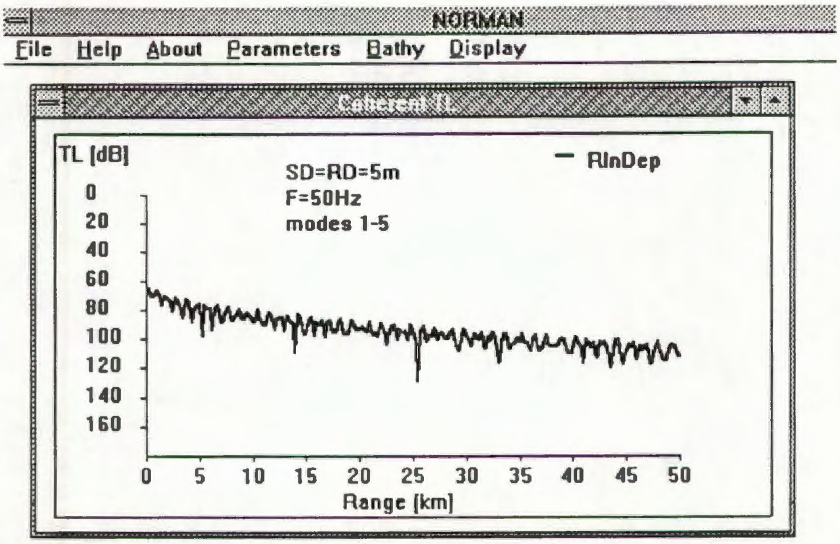

Figure 4.18: TL vs Range at 50 Hz.

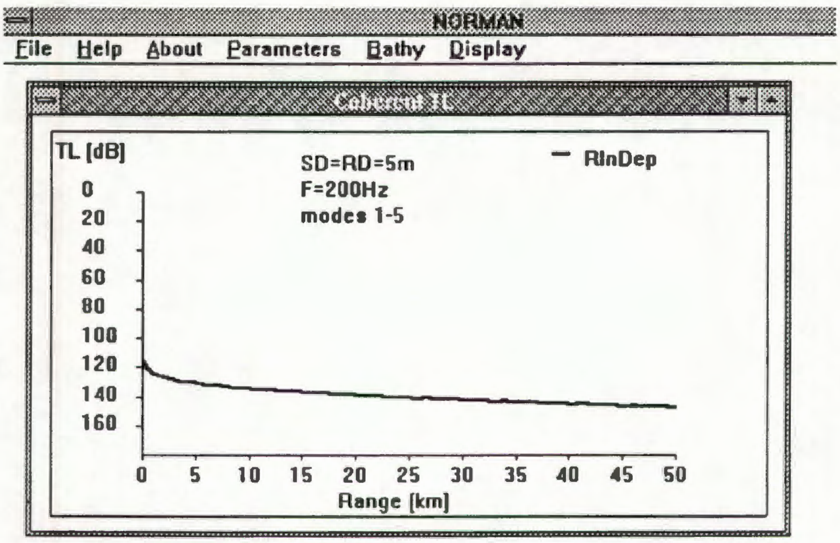

Figure 4.19: TL vs Range at 200 Hz.

4.4.3 Normal mode explanation

As important background it should be noted that this specific optimum frequency prediction was done for a downward refracting SVP (decreasing sound velocity with increasing water depth) taken off the Durban coast in shallow water in summer (see figure 3.2). This means that the minimum sound speed is located near the sea bottom and that the lowest order mode will therefore also propagate close to that depth.

An additional but very important normal mode feature now needs introduction: For any mode number n, its propagation velocity decreases with increasing frequency until a constant limit is reached. This mode property is further explained in reference [19] by Di Napoli and Middleton. The velocity limit for the lowest mode is, as is known, the minimum value of the prevailing sound velocity profile. If the mode distributions in figure 4.20 at 50 and 200 Hz for this specific downward refracting velocity profile are studied, it can be seen that the above argument is supported since the mode distribution at 200 Hz is localized closer to the bottom (sound speed minimum) than the 50 Hz distribution.

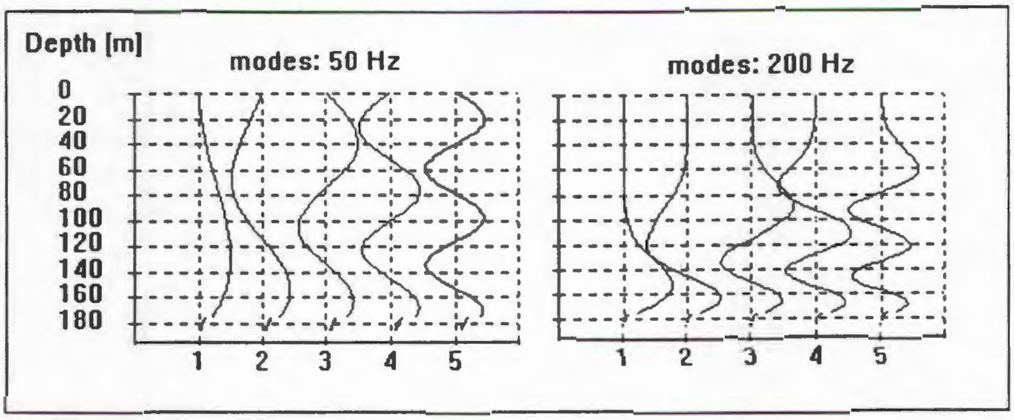

Figure 4.20: Mode distributions at 200 and 50 Hz.

Returning to sound propagation loss, the significance of the above argument becomes apparent when it is noticed that the source and receiver depth for the optimum frequency as well as the transmission loss prediction is 5 m. This implies that as the frequency is increased and the energy carrying characteristic of the mode set shifts towards the sound speed minimum (sea bottom), and thus away from the source and receiver depths, transmission loss will logically increase.

Below the optimum frequency, transmission loss also increases due to the decreasing capability of the water column to "fit" the mode distribution. Mode cut-off is therefore experienced.

4.4.4 Conclusion

The optimum frequency calculation capability of model NORMAN has been demonstrated and the mechanisms used by the environment to sustain an optimum frequency have been explained from a normal mode point of view.

4.5 Sonar application

4.5.1 Introduction

The term SONAR (SOund Navigation And Ranging) broadly describes the processes whereby underwater localisation, detection, classification and tracking of targets are done using underwater sound and the propagation principles there-of.

An active sonar uses emissions to obtain echoes re-radiating off a target, while a passive sonar listens to the radiated sound (noise) from a target. A passive sonar can also listen to emissions from a distant active source (e.g. the ATOC-FACT experiment).

The sonar equations (active and passive) govern underwater sound propagation by having terms describing the sonar itself (equipment), the target as well as the environment (medium). In this section the application of NORMAN towards predicting the performance of a passive surveillance sonar will be illustrated by a simple manipulation of the passive sonar equation.

4.5.2 The sonar problem

As a hypothetical example, a horizontal passive sonar array of hydrophones is deployed on or near the seabed in the False Bay area (Hangklip) in order to supply a surveillance capability against illegal fishing.

4.5.3 The passive sonar equation

With reference to appendix B, the essence of the sonar equations is that at the receiver the following in equality should hold:

SIGNAL (wanted) - NOISE (unwanted) $\geq$ DETECTION THRESHOLD . . . . (4.7)

The maximum allowable transmission loss value still to satisfy eq. 4.7 is called the figure-of-merit (FOM) of the system.

$$FOM = SL - [NL - DI] - DT \qquad (4.8)$$

More detail of the passive sonar equation terms can be found in appendices B and C and since the emphasis in this section is on the NORMAN application to the problem stated above, individual sonar equation terms will only be discussed briefly.

For the surveillance problem, the following realistic sonar equation terms are relevant in calculating the figure-of-merit.

TABLE 4.1:

Parameters	Value [dB] at 200 Hz
SL_{ship} @ 5 knots	115
NL Sea State 1	69
Sea State 5	80
DI (800 m array)	16
DT	-6

From table 4.1 a figure-of-merit of 68 dB for sea state 1 conditions is predicted by eq. 4.8.

4.5.4 NORMAN performance prediction

NORMAN can now be applied in order to predict a performance range for the passive seabed array, based on the allowable transmission loss (i.e. the FOM). Relevant NORMAN input data to the False Bay location can be seen in table 4.2 and figure 4.21.

TABLE 4.2:

Position	Sea State	Sea Bottom	Source depth
34°23′ S 18°42′ E	1	Mud - ρ_2, ρ_3 = 1.583 g/cm^3 - c_{CB} = 1549.5 m/s - A_2, A_3 = 0.0011 dB/Hz.m	5 m

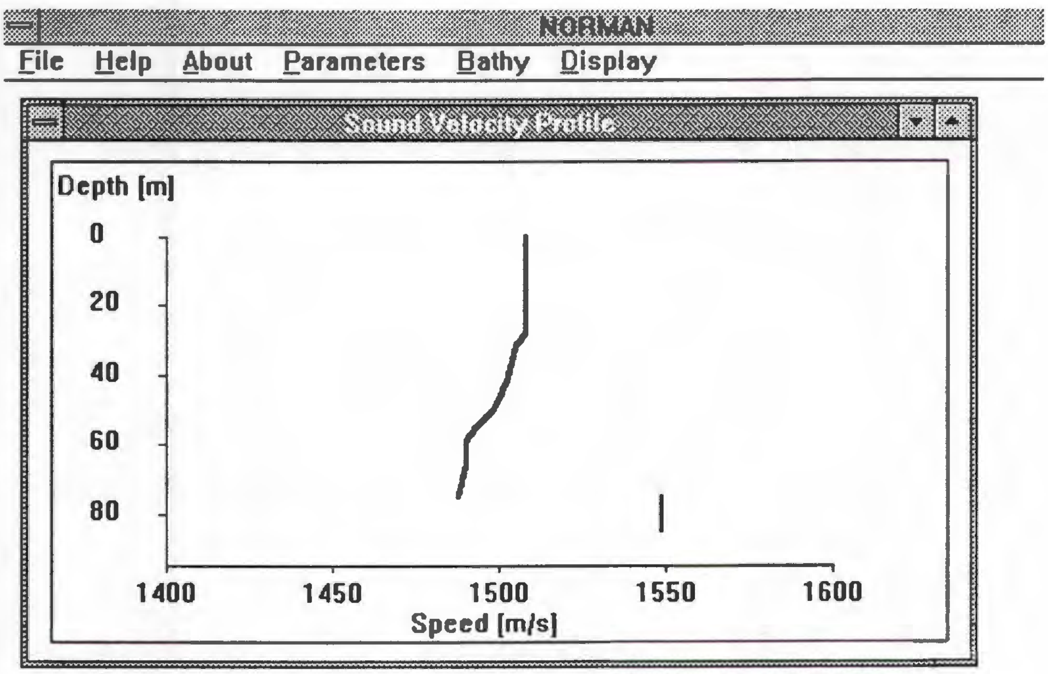

Figure 4.21: SVP in False Bay (Hangklip area, May 1990).

For a source depth of 5 m (ship) and a radiated noise frequency of 200 Hz, the acoustic field map in figure 4.22 of transmission loss values in a depth versus range frame of reference can be compiled.

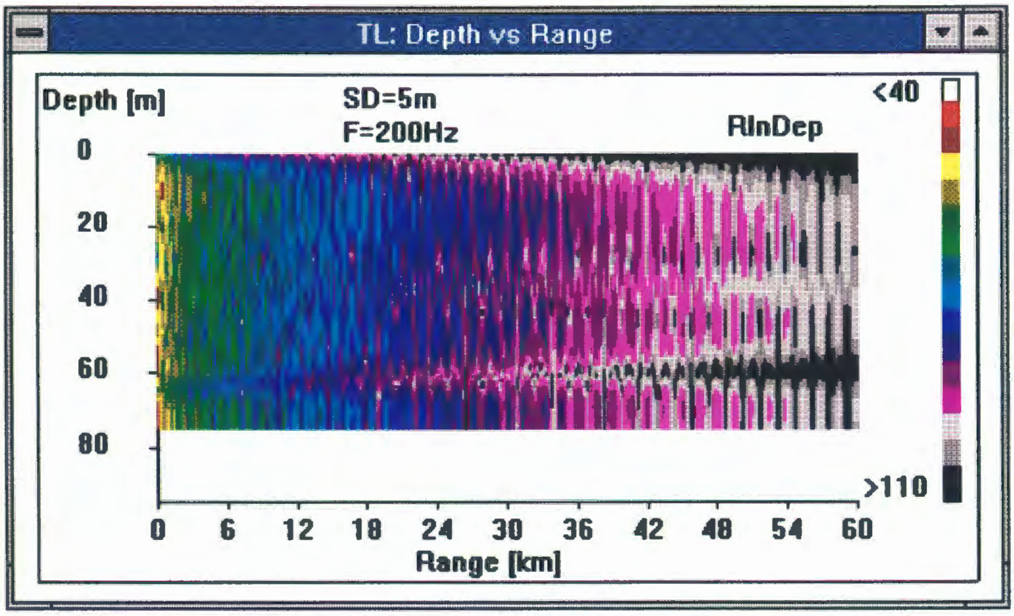

Figure 4.22: NORMAN TL: Depth vs range (False Bay, ship at 5 m, 200 Hz).

From figure 4.22 it can now be seen that a performance range of 8 km is predicted for the seabed array at 10 m off the sea bottom (Boundary between green and blue). An optimum depth can of course be designed by compiling range predictions for various receiver depths.

As a point of interest, note the sound channelling effect in range near the bottom due to the downward refracting sound velocity profile, aided by the kink in the profile at about 60 m depth.

4.5.5 Conclusion

In summary, a few observations:

- NORMAN can predict and display the characteristics of the signal field in order to be a useful tool in sonar performance prediction and therefore also in system design.

- Performance prediction is extremely environment specific and therefore, without specifying the prevailing environment and incorporating it into the model, predictions should only be taken as a guide to and not a guarantee of system performance.

4.6 Sound propagation trials

4.6.1 Introduction

Shallow water sound propagation trials, using vessel-radiated noise as an acoustic source, were held in June 1992.

The trials were conducted in False Bay on 18 June 1992 at the positions indicated in figure 4.23. While the Annie-K (IMT Workboat) was anchored in position A1, the SAS Johanna van der Merwe (Daphné-class submarine) sailed from position S1 towards position A1 on the surface, at a constant speed of 8 knots during run 1. In the second run the submarine sailed from A1 towards position S3 at the same speed. While run 1 was over a sandy bottom, run 2 was designed to involve another bottom type - in this instance mud. During both runs the submarine-radiated noise was kept as constant as possible and was recorded by means of a vertical hydrophone array as can be seen in figure 4.24.

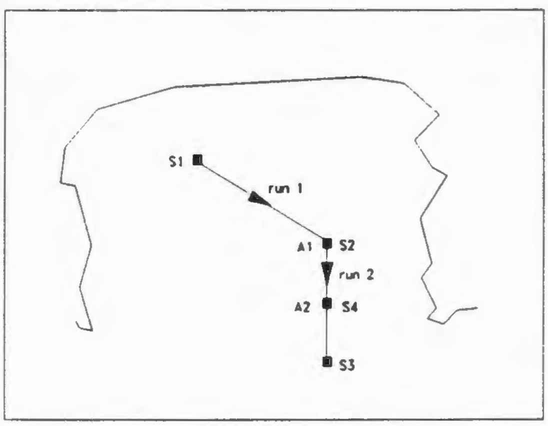

Figure 4.23: Trial position and vessel runs.

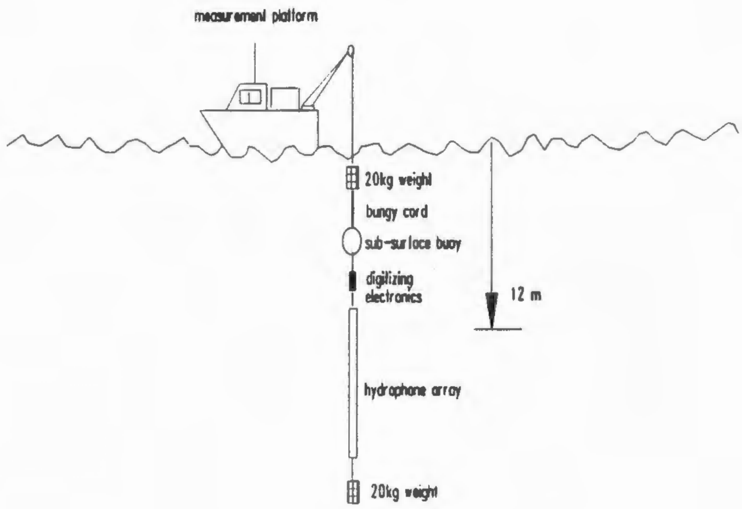

Figure 4.24: Measurement equipment deployment.

4.6.2 Measurement equipment and data display

The hydrophone array in figure 4.24 consisted of 4 sub-arrays (3 m) of 4 elements each, spaced half-wavelengths apart at 1 000 Hz.

During the two runs, 200 MByte data was digitally provided by three channels. The bottom sub-array (fourth channel) was not operational. Real-time data display in the form of a scrolling LOFAR-gram was available at sea during both runs.

4.6.3 Measurement results

From the data processing the most informative radiated signal spectral content was identified at 524 Hz for run 1 and 522 Hz for run 2. This difference in frequency is due to a Doppler shift and 523 Hz was taken as the frequency for NORMAN prediction (section 4.6.4). Transmission loss was then calculated for both runs over distances in which the signal transmission loss was separable from a background (noise) measure. These results for the two runs can be seen in figures 4.25 and 4.26.

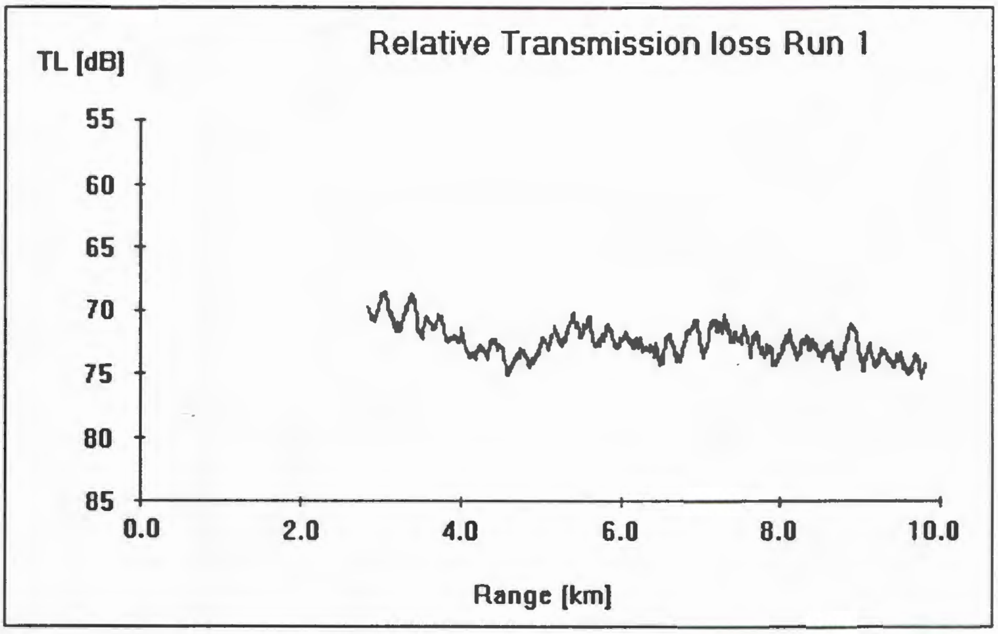

<u>Figure 4.25:</u> TL vs Range (run 1).

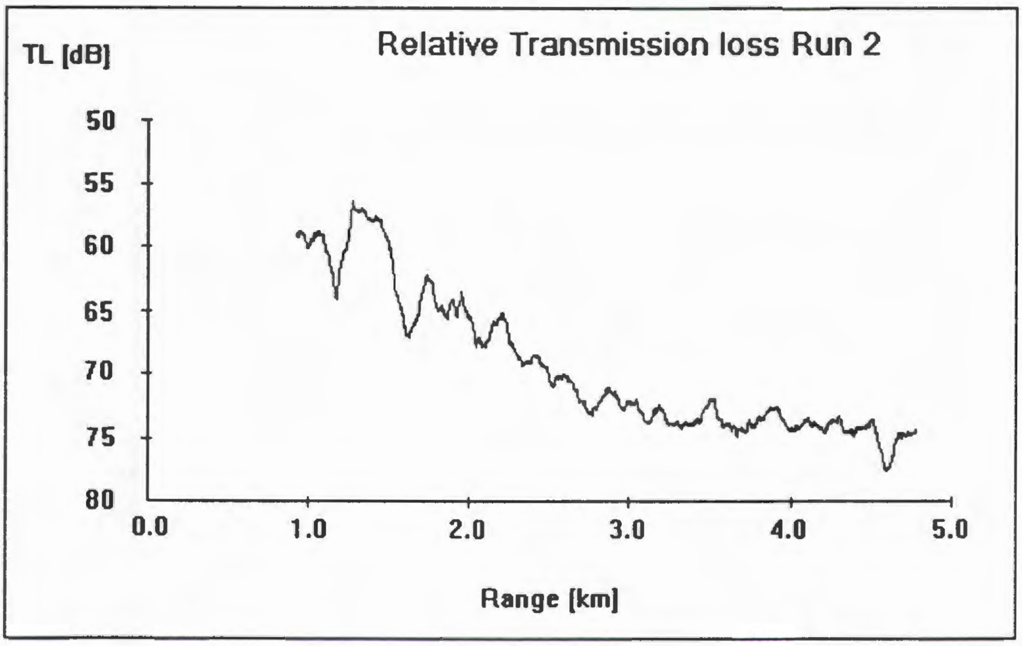

<u>Figure 4.26:</u> TL vs Range (run 2).

Since an absolute source level is not obtainable, the results in figures 4.25 and 4.26 represent relative transmission loss related to the maximum signal level (at closest range). Both results were then shifted in order to coincide with a spherical spreading law of 20 log(r) at close range. Note the good agreement between the transmission loss results for the two runs in figure 4.27. Also note the transition from spherical (20 log (r)) to cylindrical spreading (10 log(r)).

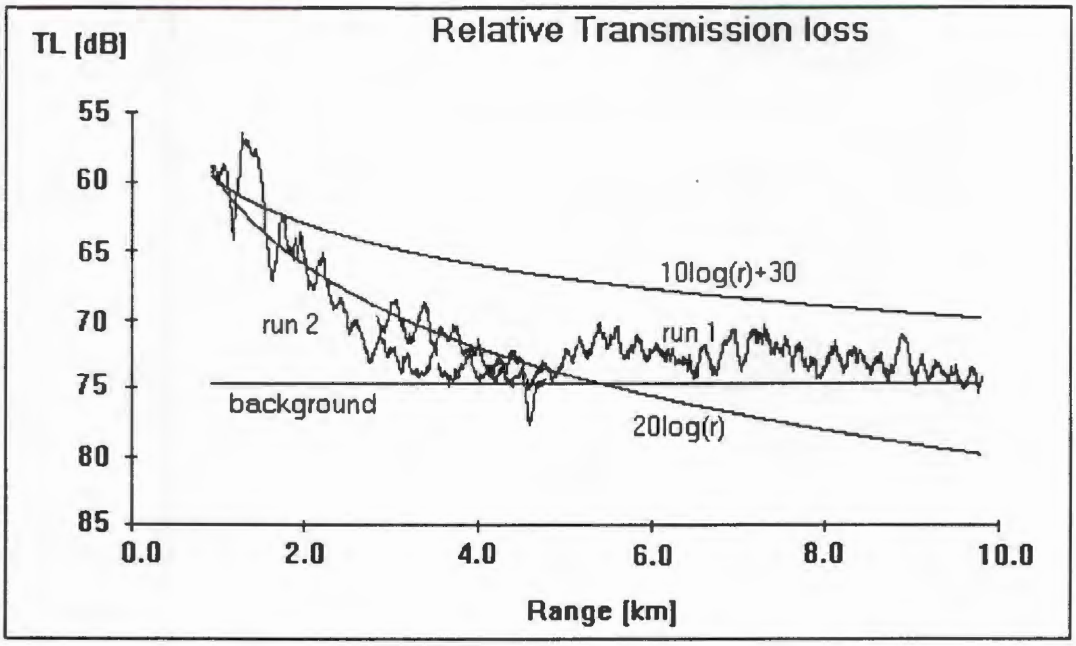

Figure 4.27: Combined TL vs Range (Runs 1 and 2).

4.5.4 NORMAN prediction vs measurement

The low frequency sound propagation measurements not only served to develop local expertise regarding low frequency measurement equipment and data processing, but also provided an opportunity to evaluate model NORMAN.

Quite a number of NORMAN transmission loss predictions are possible due to the variable sea trial environment. With reference to figure 4.23, not only does the bottom type change from positions S2 to S4, but sound velocity profiles are available for both positions S2 and S4, while the water depth also varies considerably for all positions.

It was decided to opt for two extreme cases as far as the above variability is concerned:

i. A range-independent TL prediction with only the environment at position S2 as input.

ii. A range-dependent TL prediction with two input ranges (S2 and S4), such that all possible environment variation is incorporated.

4.6.4.1 Range-independent input to NORMAN

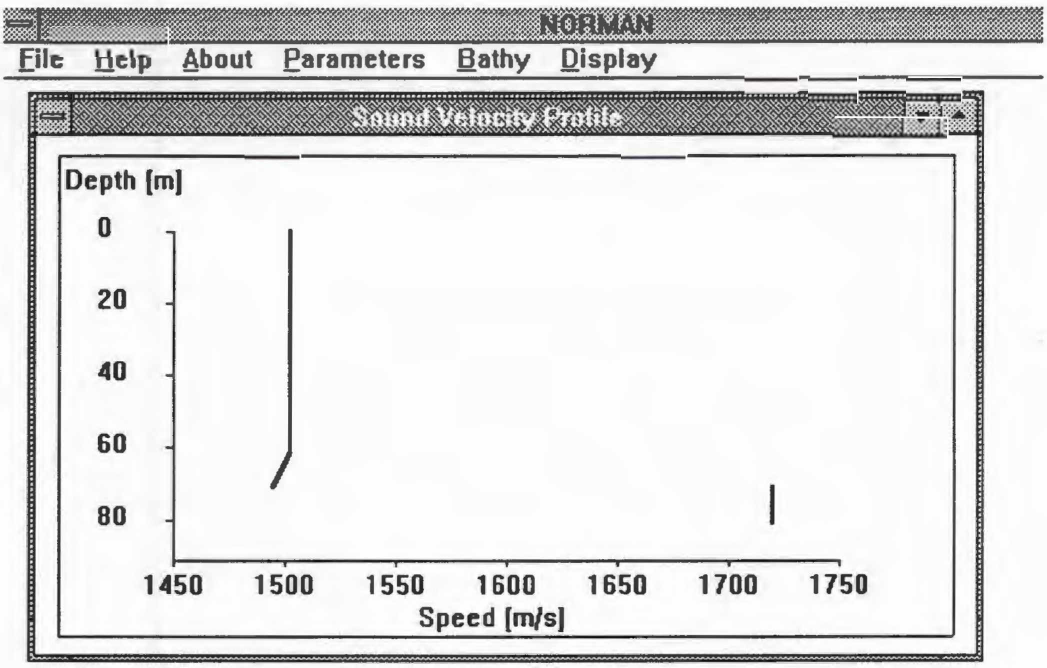

Figure 4.28: SVP at position S2 (NORMAN zero-range).

TABLE 4.3: NORMAN input in accordance with position S2.

PARAMETER	VALUE	UNIT
MODEL	FLUID	-
F	523	Hz
H_1	71	m
H_2	10	m
c_{CB}	1 720.5	m/s
zo, z	12	m
r_{min}	0	m
r_{max}	10 000	m
incr	25	m
ρ_1	1	g/cm^3
ρ_2, ρ_3	1.957	g/cm^3
NL_1	100	-
NL_2	40	-
LM	1	-
HM	20	-
A_2, A_3	0.00051	dB/Hz.m
S_o (Sea state 2)	0.5	m
Other parameters	0	-

4.6.4.2 Range-dependent input to NORMAN

While the input at zero-range (S2) remains the same as in section 4.6.4.1, a second input range at position S4 (4.5 km) provides the following additional input. Note the changes in the sound velocity profile, water depth and bottom type (i.e. density, speed, attenuation).

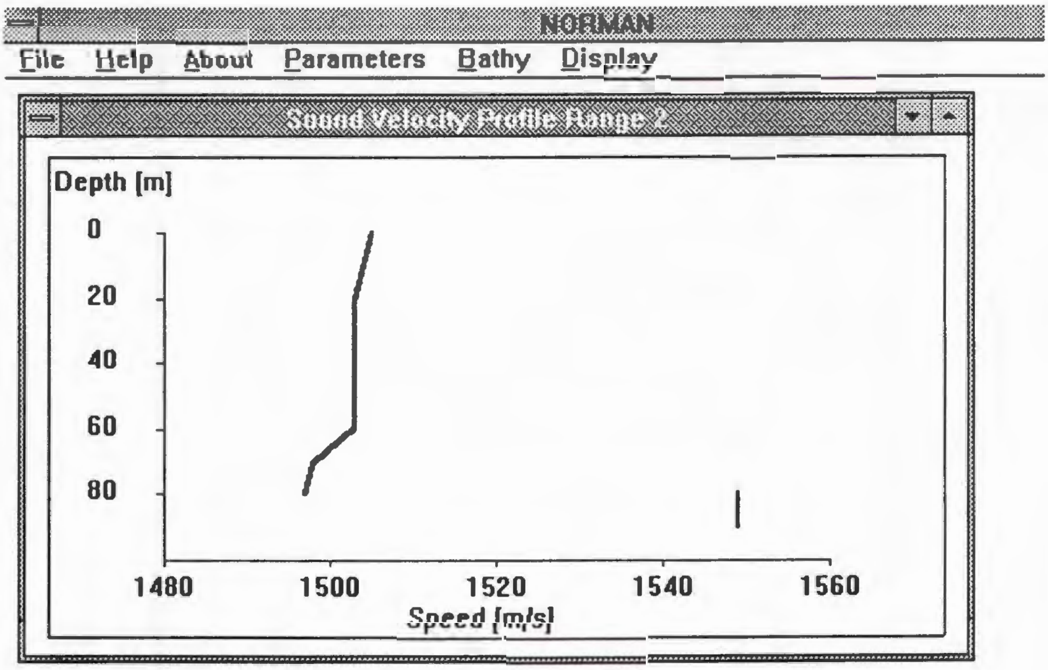

Figure 4.29: SVP at position S4.

TABLE 4.4: NORMAN input in accordance with position S4.

PARAMETER	VALUE	UNIT
MODEL	FLUID	-
F	523	Hz
H_1	84	m
H_2	10	m
c_{CB}	1 549.5	m/s
zo, z	12	m
ρ_1	1	g/cm^3
ρ_2, ρ_3	1.583	g/cm^3
NL_1	100	-
NL_2	40	-
LM	1	-
HM	20	-
A_2, A_3	0.00011	dB/Hz.m
S_o (Sea state 2)	0.5	m
Other parameters	0	-

4.6.4.2 Transmission loss versus range

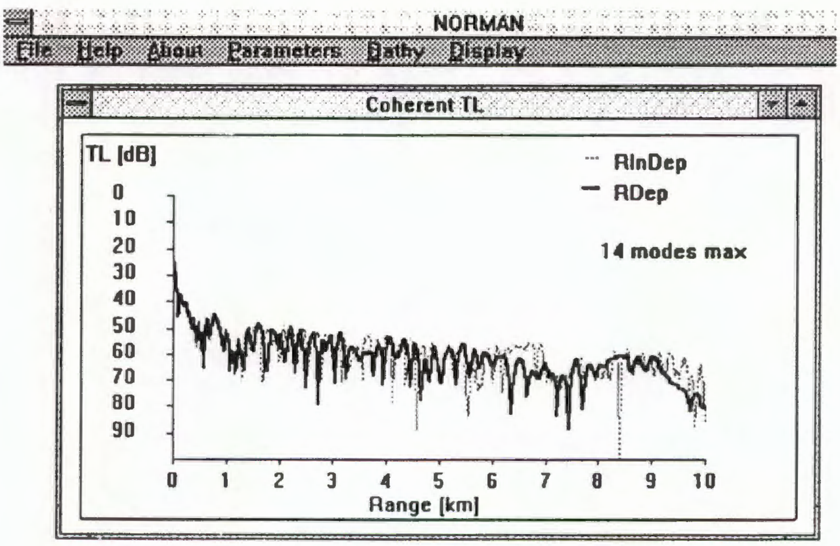

Figure 4.30: NORMAN TL vs range.

The transmission loss predictions for both the range- dependent and -independent cases can be seen in figure 4.30. As one would intuitively expect, the more absorbing mud bottom together with the increasing water depth, result in a slightly higher transmission loss prediction for the range-dependent case.

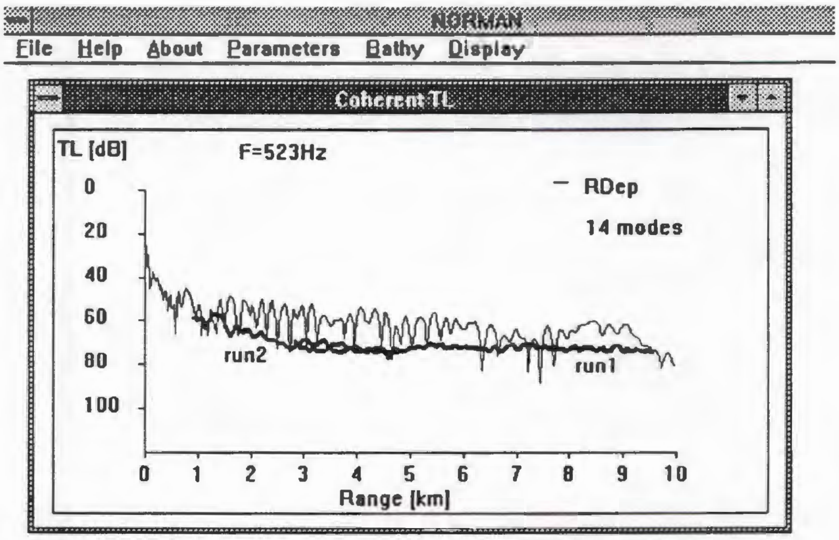

Figure 4.31: NORMAN vs measurement results.

When one now compares the range-dependent NORMAN predictions to the measurement results as can be seen in figure 4.31, the following can be remarked:

- The TL vs range-slope for measurement and prediction matches very well.
- Generally, NORMAN predicts lower TL than the relative measurements. However, the measurements were arbitrarily shifted to fit spherical spreading at 1 km (i.e. 60 dB). From figure 4.27 it does seem that a better fit to the spherical spreading law for run 2 may imply a 5 dB "down" shift. This idea is supported by the NORMAN prediction in figure 4.30 which renders a value of 55 dB at 1 km. Should the measurement results therefore have been shifted to coincide with the NORMAN prediction at 1 km, a much better model vs measurement agreement would have been obtained.

4.6.5 Conclusion

It has been shown that NORMAN can be successfully used to predict low frequency transmission loss with an acceptable degree of accuracy.

Much can however be done to extend the magnitude of the local low frequency sound propagation measurement effort. A deterministic low frequency source should also be constructed while further measurements should be conducted.

More prediction versus measurement information specifically addressing normal mode theory in shallow water can be found in reference [12].

4.7 Conclusions

It is hoped that the variety of applications which were introduced in this chapter not only served to emphasize the usefulness of the normal mode approach, but that the versatility of the specific model in handling these, were also highlighted. It is also important to note that certain basic low frequency sound propagation knowledge was necessary in order to introduce a specific application example while more knowledge was gained during the analysis process.

CHAPTER 5: CONCLUSION

In the ocean, both light and radio waves are attenuated to a far greater degree than sound. Oceanographers, seismographers and defense institutions have therefore increasingly come to appreciate the great potential of underwater acoustics as a remote sensing technique. It then naturally followed that an urgent need arose for predicting underwater sound propagation by means of a representative model.

According to Etter ([14]), the subject of underwater acoustic modelling deals with the translation of our physical understanding of sound in the sea into mathematical formulas solvable by computer. Such formulations are then intended to generalize and abstract, since a model perfectly representing reality would defeat its purpose by being as complex as the problem it is attempting to represent and solve. With the advent of the modern computer in the early seventies, the field of ocean acoustics blossomed mightily and resulted in a phenomenal growth in both the number and types of models developed over the past two decades.

While the above background do emphasize the importance as well as the existence of underwater sound propagation models as well as continous further modelling development, the local situation in the early nineties was disconcerting in this regard. The existing sound propagation models were restricted to ray theory and high frequency, while low frequency applications became increasingly important. Perhaps the biggest shortcoming was that even with the hypothetical availability of a modern low frequency model, the knowledge to operate such a model in a skilful manner was still lacking.

This thesis provides a retrospective view by documenting the effort put into erasing the identified shortcoming through realising the objectives of the study.

As a prime result of this effort, NORMAN is a low frequency underwater sound propagation software package based on normal mode theory. It was specifically developed in order to be able to investigate low frequency underwater sound propagation in the shallow water environment over the wide continental shelf south of South Africa. However, and very importantly, the result of the effort is not just a computer model, but also the acquisition of basic knowledge regarding low frequency underwater sound propagation in various specific environments. Such knowledge is vital to operating a model successfully. This belief is supported by Jensen ([5]) when he comments on sound propagation loss measurements versus predictions:

> *"However, we feel that when there is a lack of agreement it is mainly due to insufficient knowledge about the environment and not due to a lack of sophistication in the model in terms of handling the important propagation and loss mechanisms correctly."*

The approach throughout the thesis was to link *theory, modelling* and *experiment* in such a way that the original study objectives of providing a model, as well as extending the local sound propagation knowledge base, were met in a constructive manner. Special effort was therefore put into documenting as much simplified and general normal mode theory as possible, as well as to often illustrate this practically (chapters 1 and 2). Together with the specific model detail in chapter 3 it is believed that this combined information will lead to a greater local understanding of wave theory of sound propagation in the ocean, as well as to an awareness of the useful application of a model based on such theory.

With the availability of NORMAN, the studies described in this thesis have changed the local situation in respect of knowledge of and experience with low frequency underwater sound propagation in the following ways:

It now, for the first time, is possible to calculate low frequency sound propagation loss in a specified environment and to do so accurately. NORMAN's transmission loss calculation accuracy was not only benchmarked against international model output , but a NORMAN prediction measured up favourably against the results from a local low frequency sound propagation loss experiment at sea.

Not only does this model produce accurate calculations of underwater sound propagation loss, but it was also shown that now, for the first time in the local context, it is possible to study, model and predict various low frequency underwater sound propagation properties and phenomena.

- Range dependent sound propagation loss calculations can now be done. This was a basic original requirement stated in chapter 1. In the analysis of the sound propagation trial use is made of this facility and a better trial versus prediction result is obtained.

- Ducted sound propagation implies cylindrical sound spreading which is theoretically well-accounted for by the normal mode approach. This was found to be true and the concept of *virtual mode* behaviour in a surface duct was successfully investigated.

- The deep sound channel is extensively used for remote sensing and is currently of prime importance in the Global Warming programme in which South Africa is a keen participant. In this case NORMAN was used to explain the time arrival pattern measured at a receiver listening to a distant source also in the channel.

- The basic model output was also extended so that for a specific environment and for specific source and receiver positions an optimum frequency regarding sound propagation loss could be calculated.

- A low frequency sonar application was presented in which NORMAN was used to predict the maximum tolerable transmission loss which still allowed detection. Of all the terms in the sonar equation, transmission loss represents the biggest uncertainty which is now reduced, since NORMAN provides more reliable and accurate transmission loss calculations than ever were available before.

A functional low frequency sound propagation model as well as application examples are therefore now available to the local underwater acoustic community.

It should also be stressed that NORMAN, if compared to modern low frequency sound propagation models, is probably not superlative regarding presentation format, output options, complexity (e.g. 3D versus 2D) etc. The low frequency effort was however always intended to provide a basic model together with basic low frequency sound propagation knowledge. It is believed that this was achieved to such a degree that should any sophisticated model now become available for local use, enough insight will exist to operate it successfully.

In an ongoing effort however, special attention will be focused on further extending model NORMAN in order to study more arcane subjects. Ocean bottom interaction theory, signal arrival analysis, approximations to the wave equation, more sea trials and model prediction comparisons, as well as accommodating a quickly varying environment will be pursued.

Finally, the effort put into this study has been thoroughly enjoyed, with the knowledge that a practical, functional and new local analysis and research tool was established, an added bonus.

LIST OF REFERENCES

[1] Miller, J.F. and Ingenito, F., "Normal mode Fortran programs for calculating sound propagation in the ocean", NRL Memorandum Report 3071, June 1975, Naval Research Laboratory, Washington D.C., Unclassified.

[2] Miller, J.F. and Wolf, S.N., Modal Acoustic Transmission Loss (MOATL): A transmission loss computer program using a Normal-Mode model of the acoustic field in the ocean, NRL Report 8429, August 1980, Naval Research Laboratory, Washington, D.C., Unclassified.

[3] Jensen, F.B., SNAP: The Saclantcen Normal-Mode acoustic propagation model, Report SM-121, 1979.

[4] Lee, D. and McDaniel, S.T., Ocean acoustic propagation by finite difference methods, Pergamon Journals Ltd, p305-415, 1987.

[5] Jensen, F.B., Numerical models in underwater acoustics, NATO document, 1983.

[6] SD SCICON UK Ltd - Glossy, UDT-notes 1990.

[7] McDaniel, S.T., Mode-coupling due to interaction with the seabed, J. Acoust. Soc. Am. 72, p916-923, 1982.

[8] Kuperman, W.A., Models of sound propagation in the ocean, Naval Research Reviews 37(3), p32-41, 1985.

[9] Keller, J.B. and Papadakis, J.S., Wave propagation and underwater acoustics, Springer-verlag, 1st Edition, 1977.

[10] Jensen, F.B., Wave theory modelling, IEEE J. Oceanic Eng. 13 (4), p186-197, 1988.

[11] Stickler, D.C., Normal-mode program with both the discrete and branch line contributions, J. Acoust. Soc. Am. 57(4), p856-861, 1975.

[12] Ferris, R.H., Comparison of measured and calculated normal-mode amplitude functions for acoustic waves in shallow water, J. Acoust. Soc. Am 52(3), p981-988, 1972.

[13] Jensen, F.B. and Kuperman, W.A., Optimum frequency of propagation in shallow water environments, J. Acoust. Soc. Am. 73(3), p813-819, 1983.

[14] Etter, P.C., Underwater acoustic modelling, Elsevier, 1st Edition, 1991.

[15] Boyles, C.A., Acoustic waveguides, John Wiley & Sons, 1st Edition, 1984.

[16] Munk, W.H., The Heard Island experiment, Inaugural Lecture International Science Lecture Series, 1991.

[17] Guthrie, K.M., Wave theory of SOFAR signal shape, J. Acoust. Soc. Am. 56(3), p827-836, 1974.

[18] Clay, C.S. and Medwin, H., Acoustical Oceanography, John Wiley & Sons, 1st Edition, 1977.

[19] Di Napoli, F.R. and Middleton, F.H., Surface-wave propagation in a continuously stratified medium, J. Acoust. Soc. Am 39(s), p899-903, 1966.

[20] TRAY Program disk, version 5, IMT Ray Trace Model, 1992.

[21] Tolstoy, I. and Clay, C.S., Ocean acoustics : Theory and experiment in underwater sound, American Institute of Physics, 2nd Edition, 1987.

[22] Brekhovskikh, L. and Lysanov, Y., Fundamentals of ocean acoustics, Springer-Verlag, 1st Edition, 1982.

APPENDICES

APPENDIX A: ABBREVIATIONS

ATOC	Acoustic Thermometry of Ocean Climate
ATOC-FACT	Acoustic Thermometry of Ocean Climate - Feasibility Ascension Cape Town
CW	Continuous Wave
dB	Decibel
DI	Directivity Index
DT	Detection Threshold
FOM	Figure-of-Merit
GRAPES	GRid Adaptive Parabolic wave Equation Solution (PE-model)
IFD	Implicit Finite Difference-model (PE-model)
IMT	Institute for Maritime Technology
LF	Low Frequency
LOFAR	Low Frequency Analyzing and Recording
NL	Noise Level
NORMAN	NORmal Mode ANalysis
PAREQ	PArabolic EQuation (Saclant PE-model, Italy)
PE	Parabolic Equation
RD	Receiver Depth
SD	Source Depth
SL	Source Level
SOFAR	Sound Fixing and Ranging
SONAR	SOund Navigation And Ranging
SNAP	Saclantcen Normal-mode Acoustic Propagation model (Saclant, NM-mode, Italy)
SS	Sea State
SVP	Sound Velocity Profile
TL	Transmission Loss
TRAY	IMT Ray Trace Model

APPENDIX B: THE PASSIVE SONAR EQUATION

B.1 EQUATION TERMS

DI	Directivity Index
DT	Detection Threshold
FOM	Figure-of-Merit
NL	Noise Level
SL	Source Level
TL	Transmission Loss

B.2 THE PASSIVE SONAR EQUATION

$$\text{SIGNAL-NOISE} \geq \text{DETECTION THRESHOLD} \quad \text{(B.1)}$$

$$[SL\text{-}TL] - [NL\text{-}DI] \geq DT$$

$$\therefore\ TL \leq SL - [NL\text{-}DI] - DT$$

$$\Rightarrow FOM = SL - [NL\text{-}DI] - DT \quad \text{(B.2)}$$

The FOM is then the maximum allowable TL value still to satisfy the original equality in (B.1).

Note that the above terms are defined in a decibel scale so that addition and subtraction in the equation actually represent multiplication and division in the corresponding linear quantities.

APPENDIX C: GLOSSARY

Absorption:

The loss of sound intensity due to conversion of sound energy to heat (also called alpha loss).

Attenuation:

A decrease in sound pressure level due to the various los mechanisms (spreading, reflection, scattering, absorption).

Bottom loss:

A simple description of the loss encountered by a specularly reflected sound wave at the sea bottom.

Caustic:

A high concentration of sound where rays cross each other. Theory predicts an infinite high intensity due to no separation between two adjacent rays.

Decibel:

The decibel is a convenient logarithmic scale to represent sound power levels. One bel is the logarithm of a power ratio of ten. The number of decibels is ten times the number of bels.

Figure-of-Merit

The maximum transmission loss that a sonar can tolerate to achieve the required detection criteria. This is a rearrangement of the sonar formula to calculate the maximum allowable transmission loss (2TL for active, TL for passive) when all the other terms are known.

Internal wave:

Horizontal movement of ocean thermal layers causes a long period pressure wave, called an internal wave.

Isovelocity:

Of constant sound velocity.

Normal modes:

Vertical stationary waves which originate when plane wave fronts interfere due to a sound source excitation. These depth functions are complex solutions of boundary value problems encountered in solving the wave equation. Transmission loss can be calculated by evaluating a summation of normal modes.

Passive:

Mode where source radiated noise is used to gather information (e.g. surveillance).

Refraction:

This is ray bending caused by sound velocity changes (normally versus depth). A constant velocity change (gradient) bends the ray path according to an arc of a circle. The ray path satisfies Snell's law.

Shadow zone:

An area of very low sound intensity.

Shear wave:

A sound wave which propagates in or along the surface a sediment or sub bottom due to vibrational tension in the medium caused by the incident sound energy. This wave has a lower propagation velocity than the compressional wave and also experience more attenuation. The medium's ability to support shear waves is a function of density.

Shear Velocity:

The propagation speed of a shear wave.

Spreading:

Spreading of sound in space. Spreading theory are either spherical, cylindrical or no spreading. Spreading refers to sound intensity (power to area ratio).

Sound channel:

A channel in which sound is trapped and good propagation takes place. A long detection range is possible provided that the source and listener is both in the channel. The deep sound channel is called the SOFAR channel.

Surface duct:

A layer below the sea surface with increasing temperature and thus an increasing sound velocity profile that causes upward refraction towards the surface, trapping sound in the surface layer.

Surface loss:

A simple description of the loss encountered by a specularly reflected sound wave at the sea surface.

System:

The set of parameters that characterize or model the ocean and the source/receiver characteristics.

Transmission loss:

The loss in sound pressure level [dB] due to sound propagation from 1 m to the required analysis range.

APPENDIX D: COMPUTER SYSTEM AND SOFTWARE PACKAGE INFORMATION

D.1 CURRENT HARDWARE COMPUTER SYSTEM

The system which is currently being used for NORMAN computer code development and testing consists out of the following hardware components:

- 486 DX (50 MHz CPU clock speed) IBM-compatible (Err-free) mother board.
- 80387 Math co-processor.
- 4 MByte RAM.
- 80 MByte hard disc drive.
- 1.2 MByte (5.25 ") floppy disc drive.
- 1.44 MByte (3.5 ") stiffy disc drive.
- Logitech pointing device (mouse).
- Graphic and printed output either to:
    * Tatung SVGA colour monitor
    * Hewlett-Packard Laserjet III plus printer
    * Hewlett-Packard Deskjet 500 colour printer

D.2 SOFTWARE SYSTEM

The development environment is MicroSoft Windows version 3.1. This allows extended processing and a multiple output display capability. However, additional computer memory is required for this operating system in order to function properly.

The development software for generating and compiling the computer program source code is Borland Turbo Pascal for Windows version 1.5. The Borland Resource Workshop version 1.02 was used for generating the pull-down menu structure. NORMAN itself exists out of the following Turbo Pascal units which allows a logical splitting of various program functions into separately accessible blocks:

NOR_WIN	: main program
GLOBVAR	: contains global variables
DETMODE	: calculates eigenfunction
INTERVAL	: determines eigenvalues through interval reduction
MMAT	: contains various shared mathematical procedures
PLOSS	: calculates transmission loss
NORMHELP	: contains help information
VALIDIZE	: checks for valid parameter input

While NORMAN version 2 is very much a research tool under continual development, a more refined version for general distribution is planned for 1994. It is also planned to submit a summary of the current work for publication in the *Journal of Computational Acoustics* in the same year.

More information about NORMAN (NORmal Mode ANalysis) can be obtained from the author at the following address:

M. P. Stander
Institute for Maritime Technology
Simon's Town
7995
Republic of South Africa

tel: 021-7861092
fax: 021-7862189
email: "mps@msi.imt.za"

D.3 MINIMUM HARDWARE CONFIGURATION

The following computer system configuration should serve as a minimum guideline for running NORMAN to an acceptable as well as practical performance level: (Note that a lesser machine can probably cope with the mathematical processing as far as accuracy is concerned. However, when a large number of modes are present, computation time becomes the limiting factor.)

- 386 DX 25 MHz IBM-compatible machine.
- 80387 Math co-processor.
- 4 MByte RAM.
- 20 MByte hard disc drive (for on-disc Windows and Pascal).
- A 1.2 MByte floppy or a 1.44 MByte stiffy disc drive.
- Pointing device (for Windows).
- VGA colour monitor.

As an interesting comparison as well as in support of the above statement regarding the computation time restriction, table D.1 indicates the computation time difference between the current system as specified in section D.1, and the above minimum system. NORMAN was run on both systems and the acoustic fields in terms of transmission loss were calculated for the example in figure 2.5.

TABLE D.1

System	Range increments [number]	Depth increments [number]	Modes	Time [s]	Speed factor
Current	100	80	5	45	6.6
Minimum	100	80	5	295	1

From the above time difference it can therefore be concluded that the use of a slower machine than the specified minimum would be undesirable for running NORMAN.